CHEMISTRY
A European Journal

A Journal of
ChemPubSoc Europe

Accepted Article

Title: N-Heterocyclic Olefin Ligated Palladium(II) Complexes as Pre-Catalysts for Buchwald-Hartwig Aminations

Authors: Ian Watson, André Schumann, Haoyang Yu, Emma Davy, Robert McDonald, Michael Ferguson, Christian Hering-Junghans, and Eric Rivard

To be cited as: *Chem. Eur. J.* 10.1002/chem.201901376

Link to VoR: http://dx.doi.org/10.1002/chem.201901376

Supported by
ACES

WILEY-VCH

10.1002/chem.201901376

WILEY-VCH

N-Heterocyclic Olefin Ligated Palladium(II) Complexes as Pre-Catalysts for Buchwald-Hartwig Aminations

Ian C. Watson,[a] André Schumann,[b] Haoyang Yu,[a] Emma C. Davy,[c] Robert McDonald,[a] Michael J. Ferguson,[a] Christian Hering-Junghans,[b,*] Eric Rivard[a,*]

Abstract: New *N*-heterocyclic olefins (NHOs) are described with functionalization on the ligand heterocyclic backbone and terminal alkylidene positions. Various Pd(II)-NHO complexes have been formed and their use as pre-catalysts in Buchwald-Hartwig aminations was explored. The most active system for catalytic C-N bond formation between hindered arylamine and arylhalide substrates was accessed by combining various NHOs with $[Pd(cinnamyl)Cl]_2$ in the presence of NaO^tBu as a base. In these active systems our evidence suggests that catalysis is mediated by colloidal palladium metal, highlighting a different coordination ability of NHOs in comparison with commonly used *N*-heterocyclic carbene co-ligands.

Introduction

Since the discovery of bottleable *N*-heterocyclic carbenes (NHCs) by Arduengo and co-workers (Chart 1, **I**),[1] these carbon-based donors have been used with great success as ancillary ligands in metal-mediated catalysis.[2] These studies were followed by the development of abnormal *N*-heterocyclic carbenes (aNHCs, **II**) that strongly coordinate metals through anionic backbone (C4 or C5) positions.[3] Furthermore, replacement of one ring-positioned N atom in an NHC for an sp^3-hybridized carbon atom yields cyclic(alkyl)amino carbenes (CAACs, **III**), which are better π-acids when compared with NHCs (Chart 1).[4]

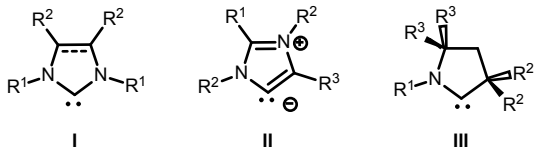

Chart 1. Generic structures of NHCs (**I**), aNHCs (**II**) and CAACs (**III**).

Owing to their strong σ-donating properties and their easily tuneable steric and electronic properties, NHCs have joined phosphines as ligands of choice in palladium-catalyzed cross-coupling reactions.[5,6] The most commonly explored Pd(II)-containing pre-catalysts for cross-coupling are outlined in Chart 2, and include the 1:1 $PdCl_2$-ligand complex (**A**),[7] palladium-allyl species (**B**),[8] and generally active "PEPPSI" complexes bearing an NHC and 3-chloropyridine (3-Cl-pyr) in a mutually *trans* orientation (**C**).[9]

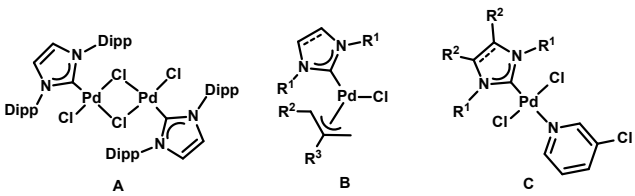

Chart 2. Widely investigated Pd(II) pre-catalysts bearing NHC co-ligands; Dipp = 2,6-^{i}Pr$_2$C$_6$H$_3$.

N-Heterocyclic olefins (NHOs) represent an emerging class of carbon-based donors that each contain a polarized, ylidic, alkylidene unit (=CH_2 or =CR_2) terminally linked to an *N*-heterocyclic carbene fragment (see Scheme 1 for contributing resonance forms).[10,11] The first isolable example of an NHO, $(MeCNMe)_2C{=}CH_2$, was described by Kuhn and co-workers in 1993,[10,11] with nucleophilic/donor ability at the terminal carbon atom demonstrated.[10-13] Moreover, *N*-Heterocyclic olefins are considered to be softer σ-donors than NHCs[13] and might yield stable coordination complexes with the soft Pd(0) centers found during cross-coupling catalysis. While the seminal work by Kuhn and co-workers introduced various NHO•$M(CO)_5$ complexes to the community (M = Cr, Mo and W),[10b] the

[a] I. C. Watson, H. Yu, Dr. R. McDonald, Dr. M. J. Ferguson, Prof. Dr. E. Rivard
Department of Chemistry
University of Alberta
11227 Saskatchewan Dr., Edmonton, Alberta, T6G 2G2, Canada
E-mail: erivard@ualberta.ca
[b] A. Schumann, Prof. Dr. C. Hering-Junghans
Leibniz Institute for Catalysis
University of Rostock
Albert Einstein Str. 29a, 18059 Rostock, Germany
[c] Prof. Dr. E. C. Davy
Department of Physical Sciences
Quest University
3200 University Boulevard, Squamish, British Columbia, V8B 0N8, Canada

Supporting information and the ORCID identification numbers for the authors of this article can be found under: *https:doi.org/10.1002/chem.xxxxxxxxx.*

number of metal complexes comprising NHOs as ligands is still limited, with examples of Au, Ir and Rh complexes now known.[12a,13-15] NHOs have also been used to stabilize reactive main group environments,[12b,16] and an exciting new direction is their use in organocatalysis.[11,17,18]

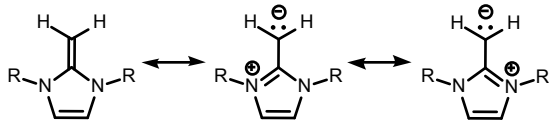

Scheme 1. Dominant canonical forms of *N*-heterocyclic olefins (NHOs).

In this paper, we describe the synthesis of new *N*-heterocyclic olefin ligands, including those bearing extended backbone π-conjugation and functionalization at the terminal alkylidene group. In addition it is shown that some NHO-Pd(II) complex combinations are viable pre-catalysts for the selective Buchwald-Hartwig C-N cross-coupling of hindered substrates, with evidence for heterogeneous catalysis modulated by Pd nanoparticles.

Results and Discussion

Synthesis of *N*-Heterocyclic Olefins (NHOs) and their Respective Pd(II) Complexes.

In a recent paper,[13] high yielding one-pot protocols were introduced to form the bulky NHOs ^{Me}IPrCH$_2$ and IPrCH$_2$ [^{Me}IPr = (MeCNDipp)$_2$C; IPr = (HCNDipp)$_2$C; Dipp = 2,6-^{i}Pr$_2$C$_6$H$_3$]. Depending on the approach used, either MeI (reaction i, Scheme 2) or the alkylchlorosilane ClCH$_2$SiMe$_3$ (reaction ii, Scheme 2) can be used as methylene sources.

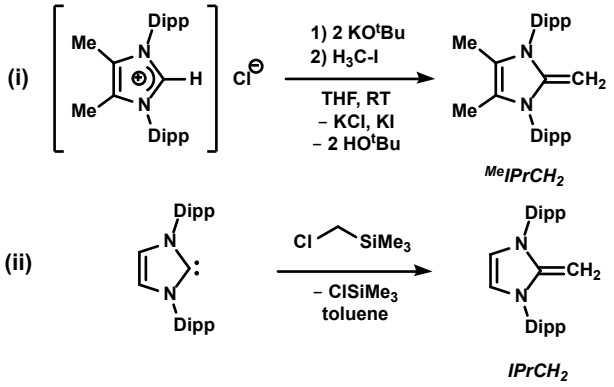

Scheme 2. Established synthetic routes towards ^{Me}IPrCH$_2$ (i, top) and IPrCH$_2$ (ii, bottom).

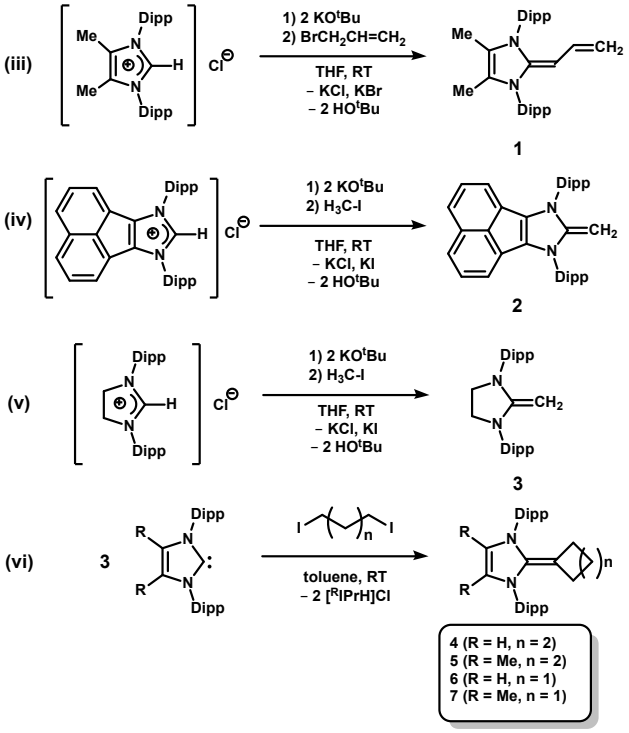

Scheme 3. Structurally modified NHOs (**1**-**7**) examined in the current study.

In order to expand the range of NHOs available and introduce possibly new (stabilizing) binding modes with late transition metals, a variety of modified NHOs were prepared (Scheme 3). For the first ligand candidate we synthesized the butadiene-NHO ^{Me}IPr=CH-CH=CH$_2$ (**1**). The structurally related species IPr=CH-CH=CH$_2$ was prepared by Jacobi von Wangelin and co-workers with nucleophilic character at the exocyclic α- and γ-C atoms postulated.[19,20] In a modified procedure, the imidazolium salt [^{Me}IPrH]Cl was combined with allyl bromide in the presence of 2 equiv. of KO^{t}Bu to give ^{Me}IPr=CH-CH=CH$_2$ (**1**) in a 84 % yield as a yellow crystalline solid (Figure 1). Placement of Me groups at the backbone of **1** was designed to suppress possible C-H activation at the 4- or 5-positions in the presence of Pd(II) complex and base; related NHO ligand activation has been recently noted by Schumann and Hering-Junghans.[21]

An *N*-heterocyclic olefin bearing a π-extended acenaphthene backbone[22] IPr(BIAN)CH$_2$ (**2**) was also prepared using a procedure analogous to that used to obtain **1** (Scheme 3). IPr(BIAN)CH$_2$ (**2**) was isolated as a deep blue air- and moisture-sensitive powder (87 % yield), and X-ray quality crystals were obtained from a benzene/hexanes mixture at 23 °C (Figure 2).[23] In a similar fashion, the saturated analogue of IPrCH$_2$, SIPrCH$_2$ (**3**) (SIPr = [(H$_2$CNDipp)$_2$C]), previously reported by Ghadwal and co-workers,[24] was obtained as a colorless crystalline solid in 70 % yield using the modified one-pot procedure outlined in Scheme 3.

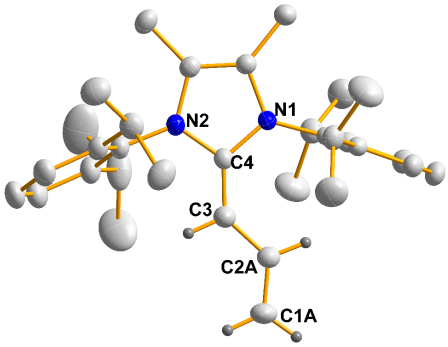

Figure 1. Molecular structure of ^{Me}IPr=CH-CH=CH$_2$ (**1**) with thermal ellipsoids shown at a 30 % probability level. Hydrogen atoms on the backbone and on the Dipp groups are omitted for clarity. Selected bond lengths [Å] and angles [°] with values belonging to a second molecule in the asymmetric unit in square brackets: C1A–C2A 1.328(3) [1.338(2)]; C2A−C3 1.411(3) [1.282(1)]; C3−C4 1.369(3) [1.369(3)]; N1−C4−N2 104.17(15) [104.17(15)]; C1A-C2A-C3 127.1(3) [125.6(11)].

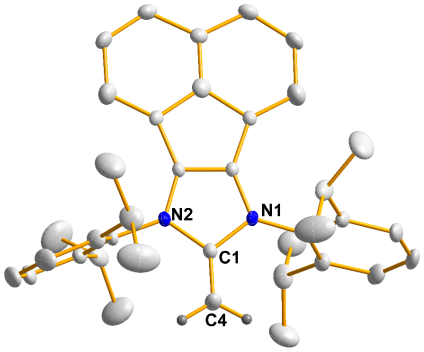

Figure 2. Molecular structure of IPr(BIAN)CH$_2$ (**2**) with thermal ellipsoids shown at a 30 % probability level. Hydrogen atoms on the backbone and on the Dipp groups are omitted for clarity. Selected bond lengths [Å] and angles [°]: C1−C4 1.336(3), N1−C1 1.405(2), N2−C1 1.403(2); N2−C1−N1 105.34(17).

The majority of the NHOs described in this study have been crystallographically characterized, and selected examples are presented in Figures 1-3.[23] ^{Me}IPr=CH-CH=CH$_2$ (**1**) shows bond alternation within the exocyclic =CH-CH=CH$_2$ group as evidenced by shorter C4-C3 [1.369(3) Å] and C2A-C1A [1.328(3) Å] distances (Figure 1) compared to the central bond C3-C2A [1.411(3) Å]. The exocyclic =CH-CH=CH$_2$ unit in **1** is in the same plane as the proximal 5-membered imidazole ring. The structure of the deep blue IPr(BIAN)CH$_2$ (**2**) was also determined by X-ray crystallography (Figure 2) and the exocyclic C1-C4 linkage [1.336(3) Å] is of a typical length for an *N*-heterocyclic olefin;[11,12b] likewise standard metrical parameters for the backbone saturated SIPrCH$_2$ (**3**) were noted (Figure S6).[23]

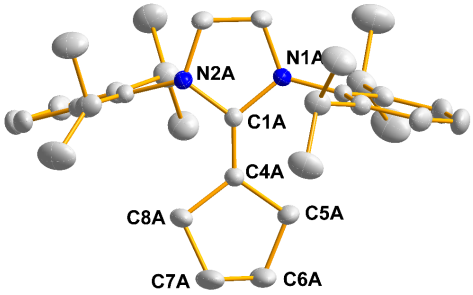

Figure 3. Molecular structure of IPr=C(CH$_2$)$_4$ (**4**) with thermal ellipsoids shown at a 30 % probability level. Hydrogen atoms are omitted for clarity. Selected bond lengths [Å] and angles [°] with values belonging to a second molecule in the asymmetric unit in square brackets: N1A−C1A 1.414(2) [1.4096(19)], N2A−C1A 1.420(2) [1.4068(19)], C1A−C4A 1.343(2) [1.353(2)]; C4A−C5A 1.522(2) [1.521(2)]; C6A−C7A 1.446(4) [1.522(2)]; N1A−C1A−N2A 103.98(13) [103.48(13)], C4A−C5A−C6A 103.65(17) [103.79(13)].

A series of NHOs bearing ring-fused cycloalkane substituents (compounds **4**-**7**, Scheme 3, reaction vi) were generated in a one-pot procedure by treatment of the requisite 1,5-diiodoalkane with three equivalents of carbene (IPr or ^{Me}IPr) in toluene. The resulting NHOs were soluble in organic solvents, facilitating their separation from the insoluble imidazolium salt by-product ([IPrH]I or [^{Me}IPrH]I) via filtration. The crystal structures of the ring-fused compounds IPr=C(CH$_2$)$_4$ (**4**) and IPr=C(CH$_2$)$_3$ (**6**) (Figures 3 and S13)[23] revealed identical ylidic C=C distances of 1.343(2) Å and 1.3432(21) Å respectively. The hydrocarbon five-membered ring (=C(CH$_2$)$_4$) in **4** is non-planar**,** while the related four-membered ring in IPr=C(CH$_2$)$_3$ (**6**) is planar. A recent theoretical study revealed a high proton affinity of ring-fused NHOs, with their basicity reaching the high-end of "superbasicity".[25]

To evaluate possible differences in donor capability amongst the NHOs **1**-**4** and **6**, computations at the B3LYP/6-31G+(d,p) level of density functional theory (DFT) were carried out.[23] As expected, these NHOs possess exocyclic double bonds with substantially polarized terminal C=C π-components, leading to accumulation of negative charge on the exocyclic carbon atom. For compounds **2** and **3** the charge on the terminal *C*H$_2$ carbon atom was computed to be −0.69e and −0.67e, respectively (as determined by a natural population analysis, NPA). In contrast, the corresponding degree of C=C bond polarization in the bicyclic NHOs **4** and **6** is less pronounced, as reflected by lower NPA charges of −0.23e and −0.24e, respectively, and almost non-polar π-components of the corresponding C=C double bonds according to Natural Bond Order (NBO) analysis (see ESI).[23] In ^{Me}IPr=CH-CH=CH$_2$ (**1**) the largest negative charge (−0.53e) is found on the terminal exocyclic carbon atom, suggesting preferential metal ligation via an end-on mode (*vide infra*).

To determine whether the bicyclic NHOs **4**-**7** introduced above were able to act as formal two-electron donors, the methylated analogue ^{Me}IPr=C(CH$_2$)$_4$ (**5**) was combined with

MeOTf. As expected, this reaction afforded the methylated salt [^{Me}IPrC(Me)(CH$_2$)$_4$]OTf (**8**) (Scheme 4 and Figure 4).

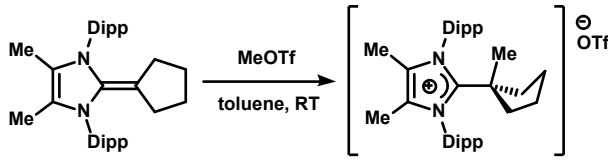

5 8

Scheme 4. The methylation of ^{Me}IPr=C(CH$_2$)$_4$ (**5**) by treatment with MeOTf.

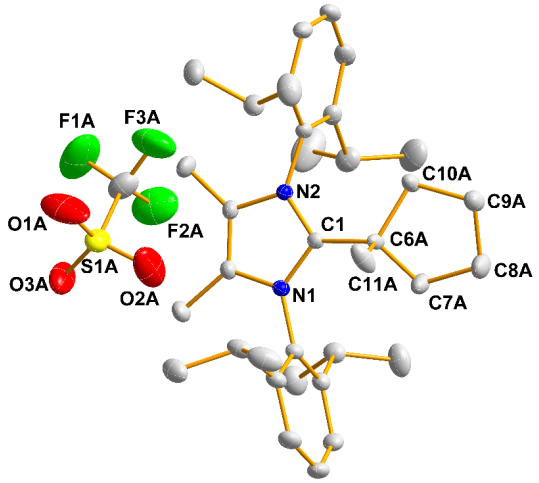

Figure 4. Molecular structure of [^{Me}IPrC(Me)(CH$_2$)4]OTf (**8**) with thermal ellipsoids shown at a 30 % probability level. Hydrogen atoms have been omitted for clarity. Selected bond lengths [Å] and angles [°]: C1−N1 1.3542(17), C1−N2 1.3526(18), C1-C6A 1.546(9); C6A-C11A 1.508(8); C8A-C9A 1.531(8); N2−C1−N1 105.85(12); C1-C6A-C11A 107.7(5); C6A-C10A-C9A 103.9(5).

^{Me}IPr=CH-CH=CH$_2$ (**1**) shows four distinct resonances for butadiene =CH-CH=CH$_2$-group with the CH proton at the vinylic position being downfield shifted compared to NHOs **2** and **3**. NHOs **1**-**7** show ^{1}H NMR resonances (in C$_6$D$_6$) consistent with the formulated structures with upfield-positioned terminal methylene =C*H*$_2$ resonances ranging from 2.42 to 2.72 ppm, with the most deshielded environment arising from the π-electron-rich NHO IPr(BIAN)CH$_2$ (**2**). The resulting ^{13}C{^{1}H} NMR shifts for the NHC-appended methylene carbon atoms (=C*R*$_2$) range from 48.3 ppm in IPr(BIAN)CH$_2$ (**2**) to 75.3 ppm for the bicyclic NHO ^{Me}IPr=C(CH$_2$)$_4$ (**5**).

With an expanded library of *N*-heterocyclic olefin ligands in hand, we then decided to explore their coordinating ability towards Pd(II) centers, with the ultimate goal of accessing suitable pre-catalysts for C-N bond formation (amination). The first example of such a complex was prepared by combining a slight molar excess of ^{Me}IPrCH$_2$ with *trans*-[Cl$_2$Pd(NCPh)$_2$] in toluene, leading to the deposition of a red crystalline precipitate. This product was identified by X-ray crystallography (Figure S20)[23] as the centrosymmetric μ-Cl-bridged dimer [(^{Me}IPrCH$_2$)PdCl(μ-Cl)]$_2$ (**9**) (Scheme 5). The most drastic structural change within the NHO ligand upon coordination is elongation of the once terminal C=C bond from a length of 1.349(2) Å[13] to a single bond C1-C4 distance of 1.453(3) Å in **9**, consistent with transfer of exocyclic C=C π-electron density from ^{Me}IPrCH$_2$ to Pd. The resulting coordinative Pd1−C4 distance of 2.026(2) Å in **9** is ca. 0.07 Å longer than in the corresponding NHC-capped PdCl$_2$ complex [(IPr)Pd(μ-Cl)]$_2$ [1.955(3) Å], which retains an similar overall geometry as in **9**.[8,26]

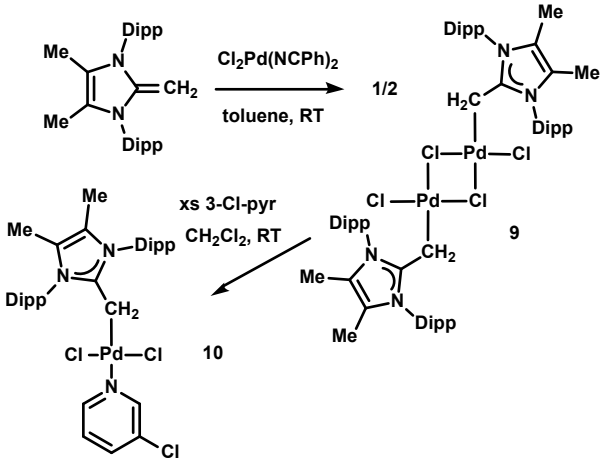

Scheme 5. Synthesis of [(^{Me}IPrCH$_2$)PdCl(μ-Cl)]$_2$ (**9**) and [(^{Me}IPrCH$_2$)PdCl$_2$(3-Cl-pyr)] (**10**).

Prior work by Organ and co-workers revealed that their (NHC)PdCl$_2$(3-Cl-pyr) "PEPPSI" complexes were active in C-N bond forming catalysis, and they selectively achieved either mono- or diarylation of primary amines (ArNH$_2$) depending on the choice of NHC and base.[27] Given the lower steric bulk of NHOs in relation to NHCs and possibly enhanced soft-soft NHO-Pd(0) interactions during catalysis, we prepared the potential pre-catalyst [(^{Me}IPrCH$_2$)PdCl$_2$(3-Cl-pyr)] (**10**) by addition of 3-chloropyridine to a solution of **9** in CH$_2$Cl$_2$ (Scheme 5). After work-up of the reaction mixture, including product recrystallization from CH$_2$Cl$_2$/hexanes (-30 °C), yellow X-ray quality crystals of [(^{Me}IPrCH$_2$)PdCl$_2$(3-Cl-pyr)] (**10**) were obtained in 67 % yield (Figure 5). The ligating Pd−C interaction in [(^{Me}IPrCH$_2$)PdCl$_2$(3-Cl-pyr)] (**10**) [2.043(6) Å] is the same within experimental error as in the pyridine-free precursor **9**, while the *trans*-disposed Pd-N$_{3\text{-Cl-pyr}}$ bond has a length [2.137(6) Å] that is similar as the related Pd-N distance of 2.137(2) Å in the *N*-heterocyclic carbene complex [(IPr)PdCl$_2$(3-Cl-pyr)].[9a]

IPr(BIAN)CH$_2$ (**2**) adopts parallel coordination chemistry as outlined for ^{Me}IPrCH$_2$, which enabled the stepwise formation of the red complex [{IPr(BIAN)CH$_2$}PdCl(μ-Cl)]$_2$ (**11**) (Figure S25)[23] and its yellow 3-chloropyridine adduct [{IPr(BIAN)CH$_2$}PdCl$_2$(3-Cl-pyr)] (**12**) (Scheme 6). The synthesis of the dimeric NHO-PdCl$_2$ adduct **11** proceeded in a low isolated yield of 31 %, and despite repeated attempts, this compound routinely contained *ca.* 10 % unknown impurities; thus the 3-chloropyridine adduct **12** was prepared from *in situ* generated **11**. Despite the change in the structure of the coordinating NHO, the

metrical parameters involving the Pd center in the IPr(BIAN)CH_2 complexes **12** were similar to its ^{Me}IPrCH_2 analogue (Figure 6). Our attempts to yield isolable Pd(II) complexes between the ring-fused NHOs **4**-**7** and Pd(II) precursors gave no reaction in each case; this observation is likely due to the small steric pocket that would result upon coordinating **4**-**7** to Pd (*vide supra*).

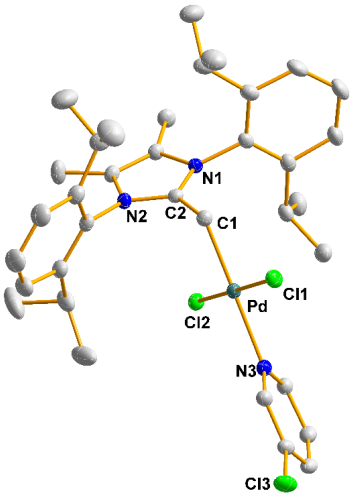

Figure 5. Molecular structure of [(^{Me}IPrCH_2)PdCl_2(3-Cl-pyr)] (**10**) with thermal ellipsoids shown at a 30 % probability level. Hydrogen atoms have been omitted for clarity. Selected bond lengths [Å] and angles [°]: N1−C2 1.354(5), N2−C2 1.351(5), C1−C2 1.448(7), Pd1−N3 2.137(6), Pd1−C1 2.043(6); N2−C2−N1 107.0(3), C2−C1−Pd1 116.7(3).

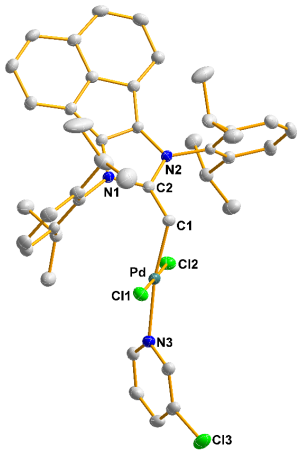

Figure 6. Molecular structure of [{IPr(BIAN)}PdCl_2(3-Cl-pyr)] (**12**) with thermal ellipsoids shown at a 30 % probability level. Hydrogen atoms have been omitted for clarity. Selected bond lengths [Å] and angles [°]: N1−C2 1.368(3), N2−C2 1.373(3), C1−C2 1.447(3), Pd1−C1 2.045(2), Pd1−N3 2.147(2); N1−C2−N2 107.41(19), C1−Pd1−N3 171.65(9), C2−C1−Pd1 120.09(17).

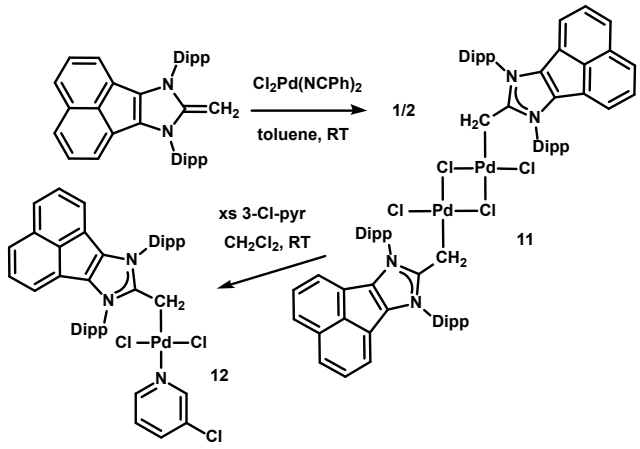

Scheme 6. Synthesis of [{IPr(BIAN)}Pd$Cl(\mu\text{-}Cl)]_2$ (**11**) and [{IPr(BIAN)}PdCl_2(3-Cl-pyr)] (**12**).

^{Me}IPr=CH-CH=CH_2 (**1**) was also complexed with Pd(II) centers in order to verify if η^1-coordination occurs via the α- or γ-position of the NHO, or whether an allyl-type η^3-coordination mode prevails. It was also hoped that during catalysis, the presence of an added olefinic unit could lead to Pd(0) complex stabilization via metal to C=C π* back-bonding. When complex **1** was combined in toluene with *trans*-[Cl_2Pd(NCPh)$_2$], the formation of a red precipitate (presumably [(^{Me}IPrCHCHCH_2)Pd$Cl(\mu\text{-}Cl)]_2$, *vide infra*) was observed. This compound was difficult to purify in a consistent fashion (*c.f.* compound **11** above), thus crude samples of this complex were subsequently combined with an excess of 3-chloropyridine to yield [(^{Me}IPrCHCHCH_2)PdCl_2(3-Cl-pyr)] (**13**) as an analytically pure red solid in a 44 % yield (Scheme 7). As shown in Figure 7, coordination of the NHO **1** to Pd is achieved through the less sterically hindered γ-position with a Pd-C distance of 2.0393(18) Å.

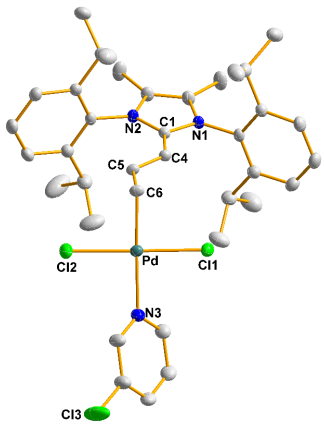

Figure 7. Molecular structure of [(^{Me}IPrCHCHCH_2)PdCl_2(3-Cl-pyr)] (**13**) with thermal ellipsoids shown at a 30 % probability level. Hydrogen atoms are omitted for clarity. Selected bond lengths [Å] and angles [°]: N1−C1 1.353(2), N2−C1 1.348(2), C1−C4 1.433(2); C4−C5 1.353(2); C5−C6 1.453(2); C6−Pd 2.0393(18); Pd−N3 2.1487(1); N2−C1−N1 106.28(13), C5−C6−Pd 103.23(12).

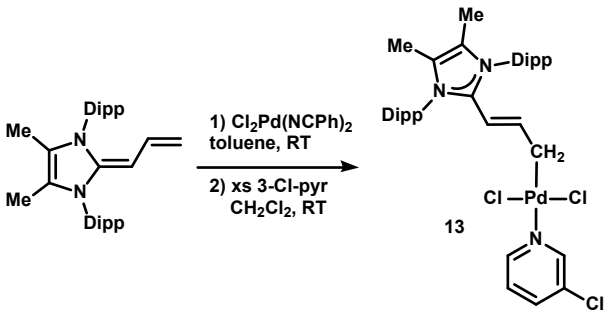

Scheme 7. Synthesis of [(^{Me}IPrCHCHCH$_2$)PdCl$_2$(3-Cl-pyr)] (**13**).

Catalytic Buchwald-Hartwig Aminations.

Motivated by the ability of (NHC)PdCl$_2$(3-Cl-pyr) complexes to act as effective pre-catalysts for cross-coupling,[9,27] we focused our initial C-N bond catalysis screening on the (NHO)PdCl$_2$(3-Cl-pyr) analogues **12** and **13**. Upon examining cross-coupling with the test substrates *p*-toluidine (4-methylaniline) and 4-chlorotoluene, no catalytic activity in the presence of the pre-catalysts **12** and **13** was observed, neither in THF, toluene, nor 1,4-dioxane. With the goal of preparing more active homogeneous Pd(0) complexes *in situ*, we explored catalyst mixtures derived from mixing the Pd sources [Pd(cinnamyl)Cl]$_2$, Pd$_2$(dba)$_3$ (dba = dibenzylideneacetone), Pd(OAc)$_2$ or PdCl$_2$ with two equivalents of the common NHO donor, ^{Me}IPrCH$_2$ in THF (80 °C, NaO^{t}Bu). As outlined in Table 1, this general procedure led to the efficient catalytic coupling of *p*-toluidine and 4-chlorotoluene. Based on an average of three runs per Pd source, it was found that the highest conversion, along with the best reproducibility, occurred with the [Pd(cinnamyl)Cl]$_2$/^{Me}IPrCH$_2$ pre-catalyst mixture (93 ± 5 % conversion after 1 hr at 80 °C). We also explored the addition of NEt$_3$ to facilitate the reduction of Pd(II) complexes to Pd(0),[28] however only marginal improvement in the case of PdCl$_2$ as a metal source was found (Table 1, entries 5 and 6).

We then set to explore the influence of different NHO ligands on the catalytic activity when partnered with [Pd(cinnamyl)Cl]$_2$ as a common Pd source (Table 2). In these trials, the influence of the saturation of the imidazole backbone (*c.f.* entry 4), on appending π-extended units (entries 2 and 5), and upon substitution at the terminal methylidene group (=CH$_2$ vs. a ring-fused =C(CH$_2$)$_4$ unit; entries 1 and 3) were examined. It was found that NHOs with an unsaturated backbone showed comparably excellent catalytic activity (> 93 % conversion after 1 hr, 80 °C, NaO^{t}Bu), with the exception of IPr(BIAN)CH$_2$, which only facilitated the coupling of *p*-toluidine with 4-chlorotoluene up to a conversion of 9 ± 2 % (Table 2, entry 5). As a result, ^{Me}IPrCH$_2$ was selected as the ligand of choice for all future cross-coupling trials as it is a commonly used NHO in our group that can be synthesized easily on a > 20 g scale. We also compared the ability of ^{Me}IPr, the NHC analogue to ^{Me}IPrCH$_2$, to perform the cross-coupling of *p*-toluidine and 4-chlorotoluene. We found that the ^{Me}IPr/[Pd(cinnamyl)Cl]$_2$ pre-catalyst system promoted the reaction quickly, with complete conversion after 20 minutes under the same conditions. The role of solvent on this cross-coupling was also explored, and it was found that THF (Table 3) consistently gave better yields for the *p*-toluidine/4-chlorotoluene coupling in relation to reactions conducted in 1,4-dioxane or toluene. It should also be mentioned that the use of pre-dried THF from a commercial solvent purification system further dried over sodium and benzophenone and distilled gave the best yields, whereas if one does not take care to exclude water/oxygen from the THF, then a lowering of conversion occurred (< 47 % yield for conditions in entry 4, Table 3).

Table 1. Optimization of palladium source for the cross-coupling of *p*-toluidine and 4-chlorotoluene.

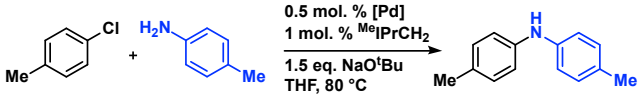

Entry	Pd source[a]	Yield [%][c]
1	[Pd(cinnamyl)$_2$Cl]$_2$	93(5)
2	Pd$_2$(dba)$_3$	85(15)
3	Pd(OAc)$_2$	41(7)
4	Pd(OAc)$_2$[a]	39(6)
5	PdCl$_2$	31(15)
6	PdCl$_2$[a]	44(4)

[a] 0.5 mol% NEt$_3$ were used [b] 1 mol% was used [c] Yield determined by ^{1}H NMR using 1,3,5-trimethoxybenzene as an internal standard. (+/-) in parentheses for triplicate runs.

Table 2. Optimization of the NHO ligand for the cross-coupling of *p*-toluidine and 4-chlorotoluene.

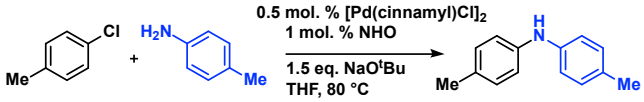

Entry	NHO[a]	Yield [%][b]
1	^{Me}IPrCH$_2$	93(5)
2	^{Me}IPrCHCHCH$_2$	96(4)
3	^{Me}IPrC(CH$_2$)$_4$	97(3)
4	SIPrCH$_2$	7(7)
5	IPr(BIAN)CH$_2$	9(2)
6	^{Me}IPr	99(1)[c]

[a] 1 mol% was used; [b] Yield determined by ^{1}H NMR using 1,3,5-trimethoxybenzene as an internal standard. (+/-) in parentheses for triplicate runs; [c] Conversion completed after 20 minutes.

After our initial catalyst screening trials led us to select [Pd(cinnamyl)Cl]$_2$/^{Me}IPrCH$_2$ as our preferred pre-catalyst for Buchwald-Hartwig aminations, we were interested in expanding the scope of this reaction. The motivating postulates behind

exploring NHOs as ligands for this chemistry were: a) the soft nature of *N*-heterocyclic olefin (NHO) donors might help stabilize Pd(0) intermediates during catalysis, and b) that the lower steric bulk of NHOs compared to *N*-heterocyclic carbenes could facilitate Pd-X/amine exchange (X = halide).[28]

Table 3. Optimization of the solvent used for the cross-coupling of *p*-toluidine and 4-chlorotoluene.

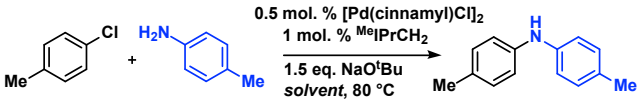

Entry	Solvent	Yield [%][a]
1	1,4-dioxane	63(2)
2	THF	93(5)
3	Toluene	17(5)
4	THF[b]	47(7)

[a] Yield determined by ^{1}H NMR using 1,3,5-trimethoxtbenzene as an internal standard. (+/-) in parentheses for triplicate runs. [b] THF not distilled from sodium and benzophenone.

We then focused our efforts on the coupling of sterically encumbered arylhalides with bulky arylamines (Scheme 8). In all cases the selective formation of secondary diarylamines occurred. For example, mesitylamine ($MesNH_2$) was coupled with 4-bromotoluene to give the mono-coupled product Mes(p-tolyl)NH in a 88 % isolated yield. We noted that further increasing the steric hindrance on the amine position resulted in invariant results. In the coupling of diisopropylaniline ($DippNH_2$) with 4-bromotoluene full conversion could not be achieved; even after heating for 2 days at 80 °C only 12% of the product Dipp(p-tolyl)NH could be isolated after purification by flash chromatography. Interestingly, the coupling of the sterically more demanding bromomesitylene (MesBr) with $DippNH_2$ proceeded smoothly, and full conversion was noted after 1 hr (as determined by ^{1}H NMR spectroscopy); after work-up, Mes(Dipp)NH was isolated in a 93 % yield. Having established the coupling of sterically demanding substrates, we turned to 9-bromoanthracene (BrAnth) to show that π-extended functional groups could be coupled. Accordingly *p*-toluidine was coupled with 9-bromoanthracene to exclusively afford the mono-coupled product N-(4-methylphenyl)anthracen-9-amine, Anth(p-tolyl)NH, in a 98 % yield. To investigate the effect of electron-donating and electron-withdrawing groups, cross-coupling was performed between 4-bromoanisole and 4-bromo-1-fluorobenzene, respectively, and 4-toluidine (Scheme 8). The yields of these reactions were 99 % and 98 %, respectively, showing that the presence of either electron-donating or electron-withdrawing groups does not hinder the effectiveness of our system. We then expanded the scope of this reaction to include the coupling of a primary alkylamine (*p*-methylbenzylamine), a secondary alkylamine (morpholine), and the secondary aniline PhNHMe with 4-chlorotoluene; in all cases, successful monocoupling was found to give the expected products in > 80 % isolated yield (Scheme 8). In order to further test the performance of our protocol, we scaled up the coupling of 4-Cl-toluene with 4-toluidine, starting from 10 mmol of the arylhalide and were able to isolate 1.84 g of di(*p*-tolyl)amine (94% yield).

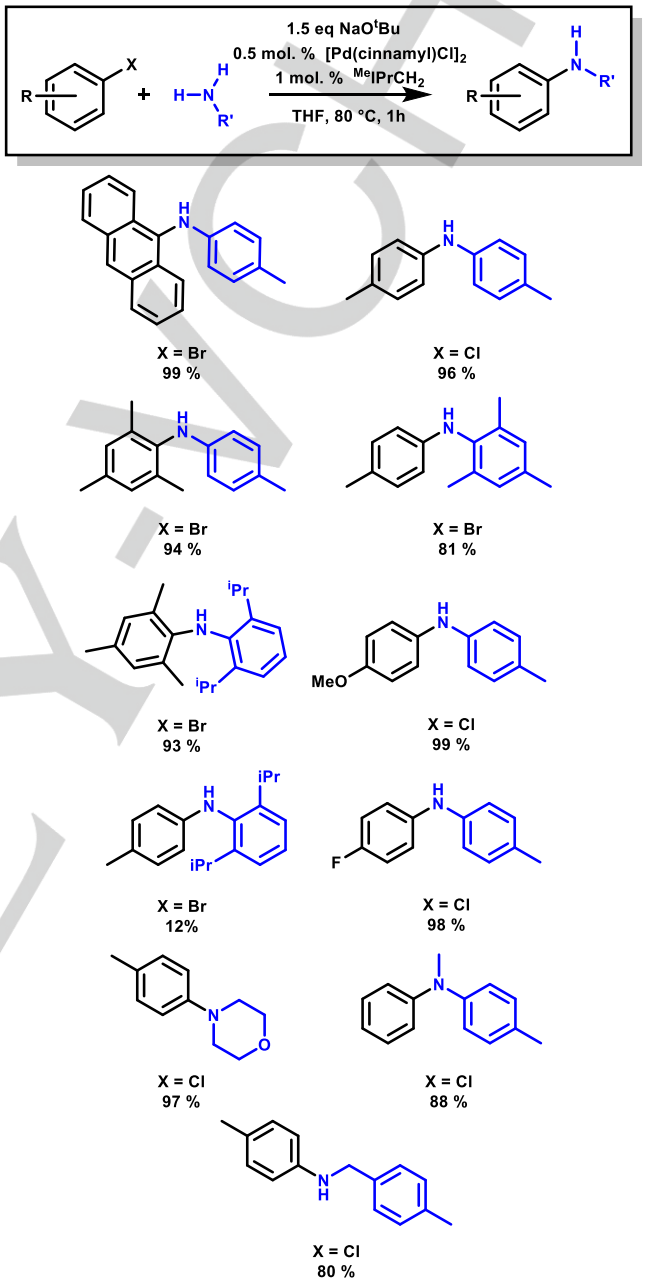

Scheme 8. The substrate scope investigated during this study. $DippNH_2$ was redistilled under vacuum prior to use. Each reaction was conducted in duplicate with average isolated yields reported (avg. deviation in yield was +/- 2 %). See Table S1 for more details.[23]

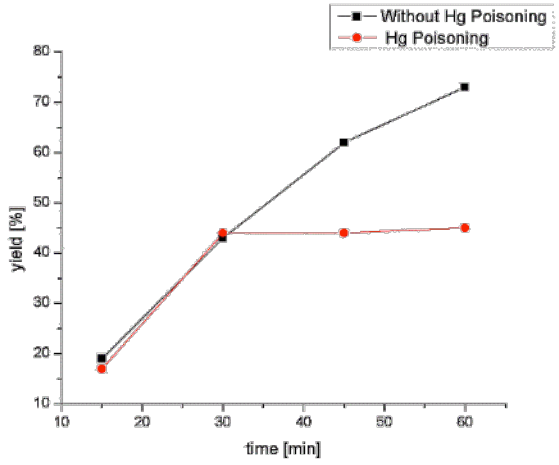

Figure 8. Plot of percent yield over time in the reaction of p-toluidine and 4-chlorotoluene at 80 °C in THF with 1.5 equiv. of NaOtBu as a base, $[Pd(cinnamyl)Cl]_2$ (0.5 mol. %) as a palladium source, and $^{Me}IPrCH_2$ (1 mol. %) as a ligand. Elemental mercury was added at time = 30 min leading to a halt in catalysis.

While the observed cessation of catalysis upon addition of Hg (Figure 8) can indicate that a mercury-palladium amalgam formed and thereby rendering catalytically active Pd nanoparticles inert, reactions involving a homogeneous Pd(0) species and mercury is also possible.[30] As such, an additional catalyst poisoning experiment using substoichiometric amounts of PMe_3 was conducted. By using substoichiometric amounts of poisoning phosphine in relation to the Pd present, further support can be offered for the presence of catalytic palladium colloids since the bulk of palladium present in these nanoparticles is buried in the core of the particles, so small amounts of poisoning ligand will halt catalysis.[31] Again, PMe_3 was added 30 minutes into the reaction time and a similar halt in catalysis was noted (Figure 9), thus adding further support for the initial presence of catalytically active Pd nanoparticles.

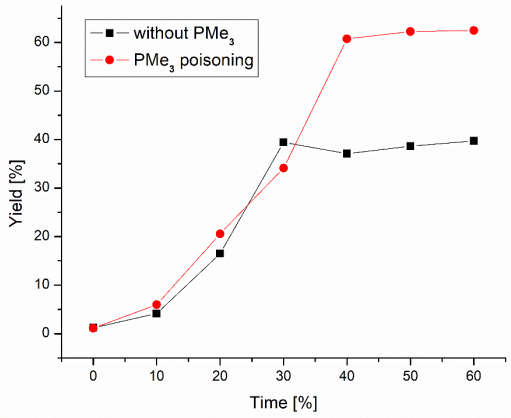

Figure 9. Plot of percent yield over time of the reaction of p-toluidine and 4-chlorotoluene at 80 °C in THF with 1.5 equiv. of NaOtBu as a base, $[Pd(cinnamyl)Cl]_2$ (0.5 mol. %) as a palladium source, and $^{Me}IPrCH_2$ (1 mol. %) as a ligand. PMe_3 was added at time = 30 min leading to a halt catalysis.

To gain a greater understanding of the system, we fitted the kinetic data to the Finke-Watzky model.[32] This model is based on a two-step process for nanoparticle formation: 1) a slow, continuous nucleation step, and 2) an autocatalytic surface growth step. This model was chosen to fit our kinetic data since it relates directly to physical properties of the reaction, yielding rate constants k_1 and k_2 with each distinct step in nanoparticle growth. Assuming that Buchwald-Hartwig amination is fast compared to these two steps, we can use the disappearance of reagent to follow nanoparticle formation.[33] As shown in Figure 10, there is reasonable agreement between the two-step Finke-Watzky model and the experimentally derived concentration of $[Pd(cinnamyl)Cl]_2$ precursor, with an R^2 value of 0.988. This suggests, in accordance with other evidence provided, that nanoparticles are being formed which, in turn, perform catalytic Buchwald-Hartwig amination. It is worth noting, however, that the induction period is not entirely flat, so there is some catalytic activity before the rate of catalysis increases. For further kinetic analyses and the plot of the concentration of 9-bromoanthracene over time, please see the *Supporting Information*.[23]

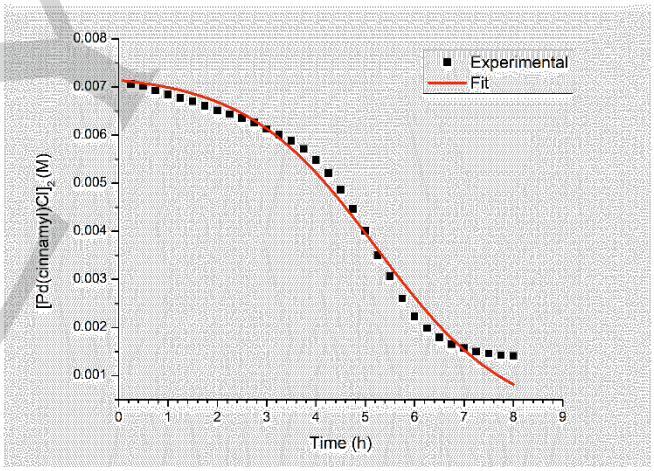

Figure 10. A plot of the concentration of $[Pd(cinnamyl)Cl]_2$ vs. time (h) during the cross-coupling of 9-bromoanthracene and *p*-toluidine as observed by *in situ* ^1H NMR spectroscopy with 1,3,5-trimethoxybenzene as an internal standard. Using the Finke-Watzky model, disappearance of pre-catalyst $[Pd(cinnamyl)Cl]_2$ and thus formation of Pd nanoparticles can be tracked by correlating the disappearance of 9-bromoanthracene. Only every third data point is shown in the plot, for clarity.

Satisfied with the evidence supporting heterogeneous catalysis, we examined the fate of the NHO ligand after palladium nanoparticle formation. One possibility would be Heck-type coupling between a tolyl group, derived from 4-chlorotoluene, and $^{Me}IPrCH_2$ ligand.[34] Accordingly, one equivalent each of $^{Me}IPrCH_2$ and 4-chlorotoluene were combined in the presence of 0.5 mol. % $[Pd(cinnamyl)Cl]_2$ and 1.5 equivalents of NaO^tBu (at 80 °C in THF); however only unreacted starting materials were found by ^1H NMR

spectroscopy. We also combined stoichiometric amounts of *p*-toluidine, 4-chlorotoluene, and ^{Me}IPrCH$_2$ with a half equivalent of [Pd(cinnamyl)Cl]$_2$ and 1.5 equivalents of NaO^{t}Bu (at 80 °C in THF). We found that the only NHO-containing species after this reaction was free ^{Me}IPrCH$_2$. This leads us to believe that the NHO is left unchanged after Pd mediated cross-coupling.

We sought to isolate the palladium nanoparticles and image them using various transmission electron microscopy (TEM) techniques. After performing the cross-coupling of *p*-toluidine and 4-chlorotoluene as per the conditions in Scheme 8, the resulting suspended Pd nanoparticles were isolated by centrifugation and washed 3 times with water to remove the sodium chloride. The resulting particles were re-suspended in anhydrous ethanol,[35] then drop-cast on a TEM grid, the solvent was then removed under vacuum followed by heating to 300 °C overnight to remove excess organic material. A control sample was prepared by drop-casting the anhydrous ethanol Pd nanoparticle suspension onto a TEM grid and removing solvent under vacuum overnight, to ensure that heating the grid did not dramatically affect the particles. The resulting spherical nanoparticles have high contrast compared to the grid, and thus were readily observable by TEM. 300 particles were measured averaging 4.80 ± 0.84 nm in size (Figures S37 to S39)[23] and are similar to the control sample prepared by vacuum drying (4.72 ± 0.91 nm). Lattice fringes with a spacing of 0.22 nm were obtained in both high-resolution and high angle angular dark-field (HAADF) scanning mode (Figure 11) and indexed to Pd [111] faces.[36] The composition of nanoparticles was further confirmed with an energy dispersive X-ray (EDX) detector. A good overlap of the nanoparticles in the dark field image with palladium signal mapping was observed (Figure S42).[23]

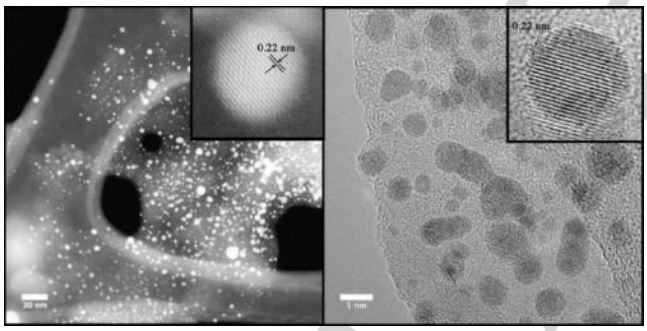

Figure 11. An HRTEM image of a Pd nanoparticle isolated after the completion of aryl amination of *p*-toluidine and 4-chlorotoluene under the conditions shown in Scheme 8. Left: An HAADF image showing Pd nanoparticles as well as their lattice fringes. Right: A STEM image depicting Pd nanoparticles and their lattice fringes.

Conclusions

A series of structurally distinct *N*-heterocyclic olefins (NHOs) have been prepared, including analogues with extended π-frameworks. In line with prior work involving NHOs, metal coordination through the terminal C atoms (η^1) was found in each case. A variety of [(NHO)PdCl$_2$(3-Cl-pyr)] complexes were prepared, however, these species proved to be ineffective in Buchwald-Hartwig cross-coupling between arylchlorides and primary arylamines. A suitable catalyst system containing Pd nanoparticles was obtained by combining the readily accessible NHO ^{Me}IPrCH$_2$ with the Pd source [Pd(cinnamyl)Cl]$_2$ in the presence of NaO^{t}Bu in THF at 80 °C. This system was active for the coupling of a wide range of arylhalides with arylamines (including high conversion with bulky substrates), while also avoiding over-arylation to tertiary triarylamines. Catalyst poisoning experiments revealed that addition of Hg or substoichiometric amounts of PMe$_3$ halts catalysis, thus pointing to the observed catalysis being heterogeneous in nature, a feature that is likely more common in cross-coupling reactions than previously noted.

Experimental Section

Materials and Instrumentation: All reactions were performed using standard Schlenk line techniques under an atmosphere of nitrogen or in an inert atmosphere glovebox (MBruan Labmaster 100). Solvents were dried using a Grubbs-type solvent purification system manufactured by Innovative Technology, Inc. and stored under an atmosphere of nitrogen and over 4 Å molecular sieves prior to use. [^{Me}IPrH]Cl,[37] [SIPrH]Cl,[38] [IPr(BIAN)H]Cl,[39] IPr,[40] ^{Me}IPr,[41] and ^{Me}IPrCH$_2$[13] were prepared according to literature procedures. [Pd(cinnamyl)(μ-Cl)]$_2$ was purchased from Sigma-Aldrich and used as received. Allyl bromide was purchased from Alfa Aesar and freeze-thaw degassed before use. NaO^{t}Bu and KO^{t}Bu were purchased from Sigma-Aldrich and used as received. 3-Chloropyridine was purchased form Oakwood Chemicals and distilled before storing in a glovebox before use. 1,5-Diiodopentane, 1,4-diiodobutane and methyl iodide were purchased from Sigma-Aldrich and freeze-thaw degassed before use. Methyl trifluoromethylsulfonate was purchased from Oakwood Chemicals and used as received. Bis(benzonitrile) palladium (II) dichloride was purchased from Strem Chemicals and used as received. ^{1}H, ^{13}C{^{1}H} and ^{19}F{^{1}H} NMR spectra were recorded on 500 MHz and 700 MHz Varian Inova spectrometers and referenced externally to SiMe$_4$ (^{1}H, ^{13}C{^{1}H}) and FCCl$_3$ (^{19}F{^{1}H}). Elemental analyses were performed by the Analytical and Instrumentation Laboratory at the University of Alberta. Melting points were measured in sealed glass capillaries under nitrogen using a MelTemp melting point apparatus and are uncorrected.

Transmission Electron Microscopy: TEM images were obtained from a JEOL JEM-ARM200CF Transmission Electron Microscope. Samples were prepared from the Buchwald-Hartwig amination of p-toluidine and 4-chlorotoluene as earlier described. Samples were centrifuged (3000 rpm, 5 min.) to separate the Pd nanoparticles from the supernatant. The isolated Pd nanoparticles were then washed 3 times with water, and then suspended in anhydrous ethanol. This suspension was then drop-cast onto a holey carbon grid, placed under vacuum for 3-4 hrs, followed by heating to 300 °C overnight to remove organic material.

X-Ray Crystallography: Crystals of appropriate quality for X-ray diffraction studies were removed from either a Schlenk tube under a stream of nitrogen, or from a vial (glove box) and immediately covered with a thin layer of hydrocarbon oil (Paratone-N). A suitable crystal was then selected, attached to a glass fiber, and quickly placed in a low-temperature stream of nitrogen. All data were collected using a Bruker APEX II CCD detector/D8 diffractometer using Mo Kα or Cu Kα radiation, with the crystal cooled to −100 °C or −80 °C, respectively. The data were

corrected for absorption through Gaussian integration from indexing of the crystal faces. Structures were solved using the direct methods programs SHELXT-2014,[42] and refinements were completed using the program SHELXL-2014.[43] Hydrogen atoms were assigned positions based on the sp^2- or sp^3-hybridization geometries of their attached carbon atoms, and were given thermal parameters 20 % greater than those of their parent atoms.

Computational Methods: Density Functional theory (DFT) calculations (full geometry optimization) were carried out on **1**-**3**, **4** and **6** starting from the geometry of their respective X-ray structures. Geometry optimizations were carried out using the Gaussian09 program package:[44] B3LYP[45] functional with a 6-31+G(d,p) basis set[46] for C, H, and N. The optimized structures were in reasonable agreement with the observed molecular structures. All stationary points were characterized by frequency analyses. For all calculated molecules and intermediates there are no imaginary frequencies. The optimized structures were also subjected to natural bond orbital (NBO) analyses using the NBO 6.0 program.[47]

Synthesis of ^{Me}IPr=CH-CH=CH$_2$ (1): To a mixture of [^{Me}IPrH]Cl (0.445 g, 0.984 mmol) and KO^{t}Bu (0.232 g, 2.07 mmol) in 10 mL of THF was added dropwise a solution of allyl bromide (0.127 g, 1.05 mmol) in 2 mL of THF. The resulting suspension was stirred at room temperature for 12 hrs. The precipitate was allowed to settle and the deep yellow supernatant was decanted away and filtered through a plug of Celite. The volatiles were evaporated under vacuum from the filtrate and the yellow residue was extracted with toluene (10 mL). Filtration of the toluene extract followed by evaporation of the toluene gave ^{Me}IPr=CH-CH=CH$_2$ (**1**) (0.285 g, 84 %) as a bright yellow solid. X-ray quality crystals of **1** were obtained by slowly evaporating a saturated hexanes solution over a period of 24 hrs at room temperature. ^{1}H NMR (500 MHz, C_6D_6): δ = 7.27-7.20 (m, 2H, Ar*H*), 7.15-7.11 (m, 4H, Ar*H*), 5.70-5.60 (m, 1H, C-C*H*=CH$_2$), 4.29 (dd, 1H, $^3J_{HH}$ = 16.1 Hz, $^2J_{HH}$ = 2.8 Hz, *cis*-CH=C*H*$_2$), 4.03 (d, 1H, $^3J_{HH}$ = 11.5 Hz, C=C*H*-CH), 3.97 (dd, 1H, $^3J_{HH}$ = 10.7 Hz, $^2J_{HH}$ = 2.8 Hz, *trans*-CH=C*H*$_2$), 3.26 (sept, 2H, $^3J_{HH}$ = 6.8 Hz, C*H*(CH$_3$)$_2$), 3.16 (sept, 2H, $^3J_{HH}$ = 6.9 Hz, C*H*(CH$_3$)$_2$), 1.52-1.47 (m, 6H, *H*$_3$C-CN), 1.43 (d, 6H, $^3J_{HH}$ = 6.8 Hz, CH(C*H*$_3$)$_2$), 1.38 (d, 6H, $^3J_{HH}$ = 6.8 Hz, CH(C*H*$_3$)$_2$), 1.18 (d, 6H, $^3J_{HH}$ = 6.9 Hz, CH(C*H*$_3$)$_2$), 1.17 (d, 6H, $^3J_{HH}$ = 6.9 Hz, CH(C*H*$_3$)$_2$). ^{13}C{^{1}H} NMR (125 MHz, C_6D_6): δ = 9.1 (H$_3$*C*-CN), 9.5 (H$_3$*C*-CN), 23.8 (CH(*C*H$_3$)$_2$), 24.1 (CH(*C*H$_3$)$_2$), 24.8 (CH(*C*H$_3$)$_2$), 28.9 (*C*H(CH$_3$)$_2$), 29.0 (*C*H(CH$_3$)$_2$), 72.2 (CH=*C*H$_2$), 95.3 (=*C*H-CH), 116.6 (N*C*-CH$_3$), 117.2 (N*C*-CH$_3$), 124.4 (Ar*C*), 124.6 (Ar*C*), 129.7 (Ar*C*), 129.8 (ArC), 132.4 (ArC), 132.6 (*C*H=CH$_2$), 134.4 (ArC), 146.0 (Ar*C*), 148.7 (ArC), 149.2 (ArC), 206.5 (N*C*N). Anal. Calcd. for $C_{28}H_{42}N_2B_2$: C, 84.16; H, 9.71; N, 6.13. Found: C, 83.49; H, 9.74; N, 5.91 %. Mp (°C): 146-149.

Synthesis of IPr(BIAN)CH$_2$ (2): [IPr(BIAN)H]Cl (0.105 g, 0.192 mmol) and KO^{t}Bu (0.044 g, 0.39 mmol) were combined in 10 mL of a 1:1 mixture of toluene/THF at room temperature and the mixture was stirred for 30 mins. To the yellow suspension was added MeI (0.031 g, 0.21 mmol) and the color immediately changed to deep blue. Stirring was continued for 12 hrs and the precipitate was allowed to settle. The supernatant was removed by filtration through a plug of Celite. The volatiles were removed from the filtrate *in vacuo* and IPr(BIAN)CH$_2$ (**2**, 0.088 g, 87 %) was obtained as a blue solid. X-ray quality crystals of **2** were obtained from a saturated benzene solution layered with hexanes at room temperature after 24 hrs. ^{1}H NMR (498 MHz, C_6D_6): δ = 7.33 (t, 2H, $^3J_{HH}$ = 7.7 Hz, Ar*H*), 7.27 (d, 4H, $^3J_{HH}$ = 7.7 Hz, Ar*H*), 7.15-7.14 (m, 2H, Napth-*H*), 6.88-6.85 (m, 2H, Napth-*H),* 6.67 (d, 2H, $^3J_{HH}$ = 7.0 Hz, Napth-*H),* 3.59 (sept, 4H, $^3J_{HH}$ = 7.0 Hz, C*H*(CH$_3$)$_2$), 2.73 (s, 2H, C=C*H*$_2$), 1.39 (d, 12H, $^3J_{HH}$ = 7.0 Hz, CH(C*H*$_3$)$_2$), 1.16 (d, 12H, $^3J_{HH}$ = 7.0 Hz, CH(C*H*$_3$)$_2$). ^{13}C{^{1}H} NMR (125 MHz, C_6D_6): δ = 24.0 (CH(*C*H$_3$)$_2$), 24.4 (CH(*C*H$_3$)$_2$), 29.2 (*C*H(CH$_3$)$_2$), 48.3 (*C*H$_2$), 118.5 (ArC), 124.8 (Ar*C*), 126.1 (ArC), 127.5 (Ar*C*), 128.9 (Ar*C*), 129.4 (Ar*C*), 129.7 (Ar*C*), 132.0 (Ar*C*), 133.5 (Ar*C*), 149.1 (Ar*C*), 157.6 (N*C*N). UV/vis (THF): λ_{max} (ε) = 286 nm (6.4 x 10^5 L mol^{-1} cm^{-1}), 406 nm (1.86 x 10^4 L mol^{-1} cm^{-1}), 686 nm (1.03 x 10^4 L mol^{-1} cm^{-1}). Anal. Calcd. for $C_{33}H_{46}N_2$: C, 86.64; H, 8.04; N, 5.32. Found: C, 86.02; H, 8.00; N, 5.17 %. Mp (°C): > 260.

Synthesis of SIPrCH$_2$ (3): A 20 mL scintillation vial was charged with [SIPrH]Cl (0.4271 g, 1.000 mmol), KO^{t}Bu (0.2468 g, 2.200 mmol) and 5 mL of THF was added. The mixture was stirred for 10 minutes, after which MeI (0.1419 g, 1.100 mmol) in 2 mL of THF was added dropwise and stirred overnight. The resulting precipitate was allowed to settle and the supernatant was filtered through a pad of Celite. The volatiles were removed from the filtrate *in vacuo* to give **3** as a white solid (0.2671 g, 70 %). X-ray quality crystals were obtained from a saturated toluene solution at -25 °C for 24 hrs. ^{1}H NMR (500 MHz, C_6D_6): δ = 7.23 (t, 2H, $^3J_{HH}$ = 7.2 Hz, Ar*H*), 7.14 (d, 4H, $^3J_{HH}$ = 7.5 Hz, Ar*H*), 3.40 (s, 4H, NC*H*$_2$), 3.37 (sept, 4H, $^3J_{HH}$ = 6.8 Hz, C*H*(CH$_3$)$_2$), 2.42 (s, 2H, C=C*H*$_2$), 1.36 (d, 12H, $^3J_{HH}$ = 6.7 Hz, CH(C*H*$_3$)$_2$), 1.27 (d, 12H, $^3J_{HH}$ = 6.7 Hz, CH(C*H*$_3$)$_2$). ^{13}C{^{1}H} NMR (126 MHz, C_6D_6): δ = 156.1 (N*C*N), 149.5 (Ar*C*), 137.2 (Ar*C*), 128.5 (Ar*C*), 124.5 (Ar*C*), 51.8 (N*C*H$_2$), 50.4 (C=*C*H$_2$), 28.7 (*C*H(CH$_3$)$_2$), 24.7 (CH(*C*H$_3$)$_2$), 24.5 (CH(*C*H$_3$)$_2$. Anal. Calcd. for $C_{28}H_{40}N_2$: C, 83.11; H, 9.96; N, 6.92. Found: C, 82.92; H, 10.07; N, 6.77 %. Mp (°C): 132-134.

Synthesis of IPr=C(CH$_2$)$_4$ (4): To a solution of IPr (0.335 g, 0.861 mmol) in 10 mL of toluene was added dropwise 1,5-diiodopentane (0.098 g, 0.30 mmol) in 2 mL of toluene. The resulting suspension was stirred at room temperature for 8 hrs. The colorless precipitate ([IPrH]I) was allowed to settle and the yellow supernatant was separated by filtration through a pad of Celite. The volatiles were removed from the filtrate under vacuum and the yellow residue was extracted with hexanes (10 mL). Evaporation of the hexanes afforded **4** (0.110 g, 84 %) as a bright yellow solid. X-ray quality crystals of **4** were obtained by slowly evaporation (under N_2) of a saturated hexanes solution over a period of 24 hrs at room temperature. ^{1}H NMR (498 MHz, C_6D_6): δ = 7.20 (t, 2H, $^3J_{HH}$ = 7.7 Hz, Ar*H*), 7.07 (d, 4H, $^3J_{HH}$ = 7.7 Hz, Ar*H*), 5.77 (s, 2H, NCH), 3.59 (sept, 2H, $^3J_{HH}$ = 6.9 Hz, C*H*(CH$_3$)$_2$), 1.80-1.73 (m, 4H, C*H*$_2$), 1.37-1.32 (m, 4H, C*H*$_2$), 1.32 (d, 12H, $^3J_{HH}$ = 7.0 Hz, CH(C*H*$_3$)$_2$), 1.25 (d, 12H, $^3J_{HH}$ = 7.0 Hz, CH(C*H*$_3$)$_2$). ^{13}C{^{1}H} NMR (125 MHz, C_6D_6): δ = 22.8 (CH(*C*H$_3$)$_2$), 25.0 (CH(*C*H$_3$)$_2$), 28.2 ((*C*H$_2$)$_4$), 28.7 (*C*H(CH$_3$)$_2$), 29.9 ((*C*H$_2$)$_4$), 75.3 (C=*C*), 116.8 (N*C*-H), 123.5 (Ar*C*), 128.7 (Ar*C*), 137.8 (Ar*C*), 138.4 (Ar*C*), 148.3 (N*C*N). Anal. Calcd. for $C_{32}H_{44}N_2$: C, 84.16; H, 9.71; N, 6.13. Found: C, 83.47; H, 9.56; N, 6.64 %. Mp (°C): 105 (dec.).

Synthesis of ^{Me}IPr=C(CH$_2$)$_4$ (5): To a solution of ^{Me}IPr (0.417 g, 1.00 mmol) in 10 mL of toluene was added dropwise 1,5-diiodopentane (0.118 g, 0.364 mmol) in 2 mL of toluene. The resulting suspension was stirred at room temperature for 8 hrs. The colorless precipitate was allowed to settle and the yellow supernatant separated by filtration through a pad of Celite. The volatiles were evaporated from the filtrate under vacuum and the yellow residue was extracted with hexanes (10 mL). Evaporation of hexanes afforded **5** (0.135 g, 77 %) as a bright yellow solid. X-ray quality crystals of **5** were obtained by placing a saturated hexanes solution in the freezer at -30 °C over a period of 24 hrs. ^{1}H NMR (498 MHz, C_6D_6): δ = 7.22 (t, 2H, $^3J_{HH}$ = 7.6 Hz, Ar*H*), 7.08 (d, 4H, $^3J_{HH}$ = 7.6 Hz, Ar*H*), 3.48 (sept, 2H, $^3J_{HH}$ = 6.9 Hz, C*H*(CH$_3$)$_2$), 1.75-1.69 (m, 4H, C*H*$_2$), 1.37 (d, 12H, $^3J_{HH}$ = 7.0 Hz, CH(C*H*$_3$)$_2$), 1.36-1.30 (m, 4H, C*H*$_2$), 1.20 (d, 12H, $^3J_{HH}$ = 7.0 Hz, CH(C*H*$_3$)$_2$). ^{13}C{^{1}H} NMR (125 MHz, C_6D_6): δ = 9.9 (NC-*C*H$_3$), 23.6 (CH(*C*H$_3$)$_2$), 24.3 (CH(*C*H$_3$)$_2$), 28.1 ((*C*H$_2$)$_4$), 28.5 (*C*H(CH$_3$)$_2$), 30.0 ((*C*H$_2$)$_4$), 73.5 (C=*C*(CH$_2$)$_2$), 116.8 (N*C*-H), 123.4 (Ar*C*), 128.7 (Ar*C*), 136.5 (Ar*C*), 139.6 (Ar*C*), 149.4 (N*C*N). Anal. Calcd. for $C_{34}H_{48}N_2$: C, 84.24; H, 9.98; N, 5.78. Found: C, 83.41; H, 9.91; N, 5.76 %. Mp (°C): 117 (dec.).

Synthesis of IPr=C(CH$_2$)$_3$ (6): To a solution of IPr (1.017 g, 2.621 mmol) in 10 mL of toluene was added dropwise 1,4-diiodobutane (0.280 g, 0.903 mmol) in 2 mL of toluene. The resulting suspension was stirred at room temperature for 12 hrs. The colorless precipitate ([IPrH]I) was allowed to settle and the yellow supernatant separated by filtration through a pad of Celite. The volatiles were removed from the filtrate under vacuum and the yellow residue was extracted with hexanes (10 mL). Evaporation of hexanes resulted afforded **6** as a solid (0.300 g, 74 %) as a bright yellow solid. X-ray quality crystals of **6** were obtained by placing a saturated hexanes solution in the freezer at -30 °C over a period of 24 hrs. ^{1}H NMR (498 MHz, C_6D_6): δ = 7.20 (t, 2H, $^3J_{HH}$ = 7.7 Hz, Ar*H*), 7.07 (d, 4H, $^3J_{HH}$ = 7.7 Hz, Ar*H*), 5.73 (s, 2H, *H*-CN), 3.53 (sept, 4H, $^3J_{HH}$ = 6.9 Hz, C*H*(CH$_3$)$_2$), 2.16 (t, 4H, $^3J_{HH}$ = 7.5 Hz, C*H*$_2$), 1.79 (quint, 2H, $^3J_{HH}$ = 7.5 Hz, C*H*$_2$), 1.41 (d, 12H, $^3J_{HH}$ = 6.9 Hz, CH(C*H*$_3$)$_2$), 1.25 (d, 12H, $^3J_{HH}$ = 6.9 Hz, CH(C*H*$_3$)$_2$). ^{13}C{^{1}H} NMR (125 MHz, C_6D_6): δ = 20.0 (*C*H$_2$), 23.0 (CH(*C*H$_3$)$_2$), 24.7 (CH(*C*H$_3$)$_2$), 28.2 (*C*H$_2$), 28.8 (*C*H(CH$_3$)$_2$), 69.7 (C=*C*(CH$_2$)$_2$), 115.6 (N*C*-H), 123.3 (Ar*C*), 128.8 (Ar*C*), 136.2 (Ar*C*), 137.2 (Ar*C*), 149.2 (N*C*N). Anal. Calcd. for $C_{31}H_{42}N_2$: C, 84.11; H, 9.56; N, 6.33. Found: C, 83.29; H, 9.62; N, 6.14 %. Mp (°C): 84 (dec.). Despite subsequent recrystallizations, an impurity of ca. 6 % free IPr was present. See Figures S14 and S15 for copies of the ^{1}H and ^{13}C{^{1}H} NMR spectra.[23]

Synthesis of ^{Me}IPr=C(CH$_2$)$_3$ (7): To a solution of ^{Me}IPr (0.133 g, 0.294 mmol) in 10 mL of toluene was added dropwise 1,4-diiodobutane (0.038 g, 0.123 mmol) in 2 mL of toluene. The resulting suspension was stirred at room temperature for 12 hrs. The colorless precipitate ([^{Me}IPrH]I) was allowed to settle and the yellow supernatant separated by filtration through a pad of Celite. The volatiles were removed from the filtrate under vacuum and the yellow residue was extracted with hexanes (5 mL) and filtered. Evaporation of the hexanes gave **7** (0.050 g, 82 %) as a bright yellow solid. ^{1}H NMR (498 MHz, C_6D_6): δ = 7.22 (t, 2H, $^3J_{HH}$ = 7.7 Hz, Ar*H*), 7.08 (d, 4H, $^3J_{HH}$ = 7.7 Hz, Ar*H*), 3.44 (sept, 4H, $^3J_{HH}$ = 7.0 Hz, C*H*(CH$_3$)$_2$), 2.11 (t, 4H, $^3J_{HH}$ = 7.5 Hz, C*H*$_2$), 1.76 (quint, 2H, $^3J_{HH}$ = 7.5 Hz, C*H*$_2$), 1.53 (s, 6H, *H*$_3$C-CN), 1.45 (d, 12H, $^3J_{HH}$ = 7.0 Hz, CH(C*H*$_3$)$_2$), 1.21 (d, 12H, $^3J_{HH}$ = 7.0 Hz, CH(C*H*$_3$)$_2$). ^{13}C{^{1}H} NMR (125 MHz, C_6D_6): δ = 9.4 (H$_3$*C*-CN), 19.7 (1C, *C*H$_2$), 23.8 (CH(*C*H$_3$)$_2$), 24.2 (CH(*C*H$_3$)$_2$), 28.6 (2C, *C*H$_2$), 28.7 (*C*H(CH$_3$)$_2$), 68.1 (C=*C*(CH$_2$)$_2$), 115.9 (N*C*-H), 123.3 (Ar*C*), 128.8 (Ar*C*), 134.6 (Ar*C*), 138.2 (Ar*C*), 149.8 (N*C*N). Anal. Calcd. for $C_{33}H_{46}N_2$: C, 84.20; H, 9.85; N, 5.95. Found: C, 83.48; H, 9.87; N, 5.69 %. Mp (°C): 108 (dec.).

Synthesis of [^{Me}IPrC(Me)(CH$_2$)$_4$]OTf (8). To a solution of ^{Me}IPr=C(CH$_2$)$_4$ (0.050 g, 0.10 mmol) in 5 mL of hexanes was added dropwise a solution of MeOTf (0.020 g, 0.12 mmol) in 1 mL of hexanes at room temperature. The resulting suspension was stirred at room temperature for 12 hrs. The colorless precipitate was isolated by filtration and washed with hexanes (2 mL). Afterwards the precipitate was dissolved in 1 mL of CH_2Cl_2 and the resulting solution layered with hexanes, which resulted in the formation of colorless X-ray quality crystals of **8** after 24 hrs at -30 °C (0.030 g, 47 %). ^{1}H NMR (399 MHz, $CDCl_3$): δ = 7.65 (t, 2H, $^3J_{HH}$ = 7.8 Hz, Ar*H*), 7.40 (d, 4H, $^3J_{HH}$ = 7.8 Hz, Ar*H*), 2.34 (sept, 4H, $^3J_{HH}$ = 6.7 Hz, C*H*(CH$_3$)$_2$), 2.08 (s, 6H, *H*$_3$C-CN), 1.56-1.30 (m, 8H, C*H*$_2$), 1.35-1.20 (m, 4H CH(C*H*$_3$)$_2$), 1.33 (d, 12H, $^3J_{HH}$ = 6.7 Hz, CH(C*H*$_3$)$_2$), 1.22 (d, 12H, $^3J_{HH}$ = 6.7 Hz, 12H, CH(C*H*$_3$)$_2$), 1.11 (s, 3H, -C*H*$_3$). ^{13}C{^{1}H} NMR (176 MHz, $CDCl_3$): δ = 10.5 (H$_3$*C*-CN), 21.1 (C-CH$_2$-*C*H$_2$), 23.5 (CH(*C*H$_3$)$_2$), 24.5 (CH(*C*H$_3$)$_2$), 25.3 (CH(CH$_3$)$_2$), 29.2 (CH(CH$_3$)$_2$), 37.4 (C-CH$_2$-CH$_2$), 46.3 (NC-*C*), 125.7 (Ar*C*), 129.9 (Ar*C*), 130.5 (Ar*C*), 132.5 (Ar*C*), 145.5 (Ar*C*), 151.4 (N*C*N). ^{19}F{^{1}H} NMR (376 MHz, $CDCl_3$): δ = -78.0 (s). Anal. Calcd. for $C_{36}H_{51}F_3N_2O_3S$: C, 66.64; H, 7.92; N, 4.32; S, 4.94. Found: C, 66.52; H, 7.92; N, 4.24; S, 4.63 %. Mp (°C): >300.

Synthesis of [(^{Me}IPrCH$_2$)PdCl(μ-Cl)]$_2$ (9): A solution of ^{Me}IPrCH$_2$ (0.053 g, 0.12 mmol) in 2 mL of toluene was added dropwise to a solution of *trans*-[Cl$_2$Pd(NCPh)$_2$] (0.035 g, 0.091 mmol) in 1 mL of toluene at room temperature. A red crystalline solid precipitated from the solution after stirring for 2 hrs. This precipitate was isolated by filtration and washed with 2 mL of fresh toluene. The collected solid was re-dissolved in a minimum amount of CH_2Cl_2 and the resulting solution was layered with hexanes. X-ray quality red crystals of **9** (0.061 g, 72 %) were then obtained after storing this layered solution at -30 °C for 24 hrs. ^{1}H NMR (498 MHz, $CDCl_3$): δ = 7.54 (t, 4H, $^3J_{HH}$ = 7.6 Hz, Ar*H*), 7.37 (d, 8H, $^3J_{HH}$ = 7.8 Hz, Ar*H*), 2.69 (sept, 8H, $^3J_{HH}$ = 6.9 Hz, C*H*(CH$_3$)$_2$), 2.42 (s, 4H, CC*H*$_2$Pd), 1.86 (s, 12H, NC-C*H*$_3$), 1.52 (d, 24H, $^3J_{HH}$ = 6.7 Hz, CH(C*H*$_3$)$_2$), 1.08 (d, 24H, $^3J_{HH}$ = 6.7 Hz, CH(C*H*$_3$)$_2$). ^{13}C{^{1}H} NMR (125 MHz, $CDCl_3$): δ = 10.2 (NC(*C*H$_3$)), 10.7 (*C*CH$_2$Pd), 25.2 (CH(*C*H$_3$)$_2$), 25.7 (CH(*C*H$_3$)$_2$), 29.0 (*C*H(CH$_3$)$_2$), 125.6 (N*C*(CH$_3$)), 129.1 (Ar*C*), 131.2 (Ar*C*), 132.4 (Ar*C*), 145.8 (Ar*C*), 146.7 (N*C*N). Anal. Calcd. for $C_{74}H_{100}N_4Pd_2Cl_4$ (**9**•2 C_7H_8): C, 63.47; H, 7.20; N, 4.00. Found: C, 62.86; H, 7.18; N, 3.96 %. Mp (°C): 163 (dec.).

Synthesis of [(^{Me}IPrCH$_2$)PdCl$_2$(3-Cl-pyr)] (10): To a solution of [(^{Me}IPrCH$_2$)PdCl((μ-Cl)]$_2$ (0.020 g, 0.014 mmol) in 2 mL of CH_2Cl_2 was added 3-chloropyridine (0.010 g, 0.08 mmol) at room temperature. Stirring was continued for 2 hrs and afterwards the volatiles were removed under vacuum. The residue was dissolved in 0.2 mL of CH_2Cl_2 and filtered through a plug of Celite. The filtrate was concentrated to incipient crystallization and layered with hexanes. After placing the sample at -30 °C for 24 hrs, pale yellow crystals of **10** formed (0.015 g, 67 %) that were suitable for X-ray crystallographic analysis. ^{1}H NMR (498 MHz, $CDCl_3$): δ = 8.62 (d, 1H, $^3J_{HH}$ = 2.2 Hz, 3-Cl-pyr), 8.54 (d, 1H, $^3J_{HH}$ = 5.4 Hz, 3-Cl-pyr), 7.57 (t, 2H, $^3J_{HH}$ = 7.8 Hz, Ar*H*), 7.56-7.53 (m, 1H, 3-Cl-pyr), 7.39 (d, 4H, $^3J_{HH}$ = 7.8 Hz, Ar*H*), 7.09 (dd, 1H, $^3J_{HH}$ = 8.0 Hz, $^3J_{HH}$ = 5.7 Hz, 3-Cl-pyr), 2.60 (sept, 4H, $^3J_{HH}$ = 6.7 Hz, C*H*(CH$_3$)$_2$), 2.60 (s, 2H, CC*H*$_2$-Pd), 1.96 (s, 6H, NC-C*H*$_3$), 1.44 (d, 24H, $^3J_{HH}$ = 6.7 Hz, CH(C*H*$_3$)$_2$), 1.13 (d, 12H, $^3J_{HH}$ = 6.7 Hz, CH(C*H*$_3$)$_2$). ^{13}C{^{1}H} NMR (126 MHz, $CDCl_3$): δ = 10.4 (NC(*C*H$_3$)), 25.0 (CH(*C*H$_3$)$_2$), 25.3 (CH(*C*H$_3$)$_2$), 28.8 (*C*H(CH$_3$)$_2$), 124.2 (Ar*C*), 125.5 (Ar*C*), 126.1 (Ar*C*), 129.9 (Ar*C*), 131.2 (Ar*C*), 136.6 (Ar*C*), 146.8 (Ar*C*), 149.4 (Ar*C*), 150.5 (Ar*C*), 163.8 (N*C*N). Anal. Calcd. for $C_{34}H_{45}Cl_3N_3Pd$: C, 58.26; H, 6.43; N, 5.80. Found: C, 58.51; H, 6.20; N, 5.82 %. Mp (°C): 178 (dec).

Synthesis of [[{IPr(BIAN)CH$_2$}PdCl(μ-Cl)]$_2$ (11): A solution of IPr(BIAN)CH$_2$ (0.063 g, 0.12 mmol) in 2 mL of toluene was added dropwise to a solution of *trans*-[Cl$_2$Pd(NCPh)$_2$] (0.046 g, 0.12 mmol) in 1 mL of toluene at room temperature. A red crystalline solid precipitated from the solution after stirring for 2 hrs. The precipitate was isolated by filtration and washed with 2 mL of fresh toluene. The collected solid was re-dissolved in a minimum amount of CH_2Cl_2, and the resulting solution was layered with hexanes. X-ray quality red crystals of **11** (0.030 g, 31 %) were obtained from this layered solution after cooling at -30 °C for 24 hrs. Despite obtaining crystalline material, the bulk sample routinely contained *ca.* 10 % impurity (Figure S26).[23] ^{1}H NMR (498 MHz, $CDCl_3$): δ = 7.84 (d, 4H, $^3J_{HH}$ = 6.9 Hz, Naph-*H*), 7.82 (t, 4H, $^3J_{HH}$ = 7.9 Hz, Ar*H*), 7.59 (d, 8H, $^3J_{HH}$ = 7.9 Hz, Ar*H*), 7.46 (dd, 4H, $^3J_{HH}$ = 6.9 Hz, $^3J_{HH}$ = 8.1 Hz, Naph-*H*), 7.02 (d, 4H, $^3J_{HH}$ = 6.9 Hz, Naph-*H*), 2.95 (sept, 8H, $^3J_{HH}$ = 6.9 Hz, C*H*(CH$_3$)$_2$), 2.57 (s, 4H, CC*H*$_2$-Pd), 1.49 (d, 24H, $^3J_{HH}$ = 6.7 Hz, CH(C*H*$_3$)$_2$), 0.98 (d, 24H, $^3J_{HH}$ = 6.7 Hz, CH(C*H*$_3$)$_2$).

[{IPr(BIAN)CH$_2$}PdCl$_2$(3-Cl-pyr)] (12): To a solution of crude [{IPr(BIAN)CH$_2$}PdCl(μ-Cl)]$_2$ (0.034 g, 0.021 mmol) in 2 mL of CH_2Cl_2 was added 3-chloropyridine (0.015 g, 0.13 mmol) at room temperature. Stirring was continued for 2 hrs and the solvent was then removed under vacuum. The residue was dissolved in 0.2 mL CH_2Cl_2 and filtered through a plug of Celite. The filtrate was concentrated to incipient crystallization and layered with hexanes. After placing the sample at -30 °C for 24 hrs **12** (0.012 g, 32 %) was obtained in the form of yellow crystals suitable for X-ray crystallographic analysis. ^{1}H NMR (498 MHz,

$CDCl_3$): δ = 8.80 (d, 1H, $^3J_{HH}$ = 2.4 Hz, 3-Cl-pyr), 8.70 (dd, 1H, $^3J_{HH}$ = 5.5, $^3J_{HH}$ = 1.4 Hz, 3-Cl-pyr), 7.81 (d, 2H, $^3J_{HH}$ = 8.2 Hz, Naph-*H*), 7.69 (t, 2H, $^3J_{HH}$ = 7.9 Hz, Ar*H*), 7.56-7.53 (m, 1H, 3-Cl-pyr), 7.50 (d, 4H, $^3J_{HH}$ = 7.9 Hz, Ar*H*), 7.40 (dd, 2H, $^3J_{HH,1}$ = 8.2 Hz, $^3J_{HH,1}$ = 7.0 Hz, Naph-*H*), 7.11 (dd, 1H, $^3J_{HH}$ = 8.1 Hz, $^3J_{HH}$ = 5.5 Hz, 3-Cl-pyr), 7.02 (d, 2H, $^3J_{HH}$ = 7.0 Hz, Naph-*H*), 3.15 (sept, 8H, $^3J_{HH}$ = 6.9 Hz, C*H*$(CH_3)_2$), 2.86 (s, 4H, CCH_2-Pd), 1.44 (d, 12H, $^3J_{HH}$ = 6.7 Hz, CH(CH_3)$_2$), 1.01 (d, 12H, $^3J_{HH}$ = 6.7 Hz, CH(CH_3)$_2$). $^{13}C\{^1H\}$ NMR (126 MHz, $CDCl_3$): δ = 23.9 (CH(*C*H_3)$_2$), 25.8 (CH(*C*H_3)$_2$), 29.4 (*C*H$(CH_3)_2$), 122.6 (Naph-*C*), 124.3 (pyr-*C*), 127.7 (Naph-*C*), 129.2 (Ar*C*), 129.8 (Ar*C*), 129.9 (Ar*C*), 130.9 (Naph-*C*), 132.0 (Ar*C*), 131.7 (Ar*C*), 132.0 (Ar*C*), 136.6 (pyr-*C*), 146.6 (pyr-*C*), 149.6 (pyr-*C*), 150.7 (pyr-*C*), 168.3 (N*C*N). Anal. Calcd. for: C, 63.71; H, 5.67; N, 5.14. Found: C, 61.72; H, 5.65; N, 5.01. Despite repeated attempts, combustion analysis gave consistently low carbon values; see Figures S27-S28 for copies of the NMR spectra.[23] Mp (°C): 183-185 (dec.).

[(^{Me}IPrCHCHCH$_2$)PdCl$_2$(3-Cl-pyr)] (13): A solution of ^{Me}IPr=CH-CH=CH_2 (0.110 g, 0.241 mmol) in 1 mL toluene was added dropwise a solution of *trans*-[Cl_2Pd(NCPh)$_2$] (0.070 g, 0.18 mmol) in 5 mL of toluene at room temperature. After 2 hrs a red precipitate formed, which was isolated by filtration and washed with 2 mL of toluene. This solid was then dissolved in 1 mL of CH_2Cl_2 and 3-chloropyridine (0.027 g, 0.24 mmol) was then added. The resulting mixture was filtered through Celite and the volatiles were removed *in vacuo* from the filtrate. The crude product was then recrystallized from an acetonitrile/hexanes mixture that was cooled to -30 °C for 24 hrs, affording red X-ray quality crystals of **13** (0.0712 g, 46 %). ^{1}H NMR (498 MHz, $CDCl_3$): δ = 8.86 (br, 1H, 3-Cl-pyr), 8.76 (br, 1H, 3-Cl-pyr), 7.63 (t, 2H, $^3J_{HH}$ = 8.0 Hz, Ar*H*), 7.57 (d, 1H, $^3J_{HH}$ = 8.0 Hz, 3-Cl-pyr, br), 7.42 (d, 4H, $^3J_{HH}$ = 8.0 Hz, Ar*H*), 7.13 (br, 1H, 3-Cl-pyr), 6.08-5.99 (m, 1H, CH=C*H*), 5.92 (d, 1H, $^3J_{HH}$ = 15.5 Hz, C*H*=CH), 3.01 (d, 2H, $^3J_{HH}$ = 9.3 Hz, CHCH_2Pd), 2.45 (sept, 4H, $^3J_{HH}$ = 6.9 Hz, C*H*$(CH_3)_2$), 1.98 (s, 6H, NCCH_3), 1.36 (d, 12H, $^3J_{HH}$ = 7.0 Hz, CH(CH_3)$_2$), 1.25 (d, 12H, $^3J_{HH}$ = 7.0 Hz, CH(CH_3)$_2$). $^{13}C\{^1H\}$ NMR (125.7 MHz, $CDCl_3$): δ = 9.4 (NCCH_3), 19.7 (CH=CH-*C*H_2), 23.8 (CH(*C*H_3), 24.3 (CH(*C*H_3)$_2$), *C*H$(CH_3)_2$, 29.2 (*C*H$(CH_3)_2$, 97.7 (*C*H=CH-CH_2), 125.3 (3-Cl-pyr), 125.7 (Ar*C*), 128.6 (3-Cl-pyr), 132.2 (Ar*C*), 145.2 (3-Cl-pyr), 146.3 (3-Cl-pyr), 156.8 (CH=*C*H-CH_2). Anal. Calcd. for $C_{51}H_{39}Cl_3N_3Pd$: C, 59.14; H, 6.57; N, 5.61. Found: C, 59.14; H, 6.57; N, 5.79. Mp(°C): 154-156 (dec).

Buchwald-Hartwig Cross-Coupling Procedure: Preparation of the reaction mixtures were conducted in a glovebox under an argon atmosphere. A 0.100 M stock solution of ^{Me}IPrCH_2 and a 0.0125 M stock solution of [Pd(cinnamyl)Cl]$_2$ were prepared. To a mixture of 1.00 mmol arylhalide, 1.20 mmol arylamine and 144 mg (1.50 mmol) NaO^{t}Bu in 2 mL of THF in a vial was added 100 µL (0.0100 mmol) of the ^{Me}IPrCH_2 stock solution and 400 µL (0.00500 mmol) of the [Pd(cinnamyl)Cl]$_2$ stock solution were added. Molecular sieves (4 Å) were added and the vial was capped using a cap with a PTFE septa. The reaction mixture was stirred for 1 hr at 80 °C. The reaction mixture was sampled via syringe for NMR analysis. To isolate the product, after cooling to room temperature the vial was opened to air, filtered, then evaporated using a rotary evaporator. The products were isolated by column chromatography (silica, n-hexane/ethyl acetate 10:1) or flash chromatography (silica, n-hexane eluent).[23]

Acknowledgements

This work was supported by the donors of The American Chemical Society Petroleum Research Fund (ACS-PRF), the Canada Foundation for Innovation, the Faculty of Science at the University of Alberta, and the Natural Sciences and Engineering Research Council (NSERC) of Canada (Discovery and CREATE grants to E.R.; CREATE fellowship to I.W.). E.R. also thanks the Alexander von Humboldt Foundation for a fellowship. C. H.-J. thanks Prof. M. Beller for his support, the Alexander von Humboldt Foundation for funding (Returning Fellowship) and the Max Buchner Research Foundation for a fellowship. Sean Liew and Kate Powers are also acknowledged for early synthetic work on this project. Prof. Rylan Lundgren (University of Alberta) is also acknowledged for helpful advice.

Keywords: N-Heterocyclic olefins • Buchwald-Hartwig amination • Pd complexes • Nanoparticle catalysis

[1] A. J. Arduengo, R. L. Harlow, M. Kline, *J. Am. Chem. Soc.* **1991**, *113*, 361-363.

[2] S. P. Nolan, C, Cazin, Science of Synthesis: N-Heterocyclic Carbenes in Catalytic Organic Synthesis, Vol. 1 (Eds.: S. P. Nolan, C. Cazin), Thieme Gruppe, Stuttgart, pp 161-182.

[3] a) S. Gründemann, A. Kovacevic, M. Albrecht, J. W. Faller, R. H. Crabtree, *J. Am. Chem. Soc.* **2002**, *124*, 10473−10481; b) H. Lebel, M. K. Janes, A. B. Charette, S. P. Nolan, *J. Am. Chem. Soc.* **2004**, *126*, 5046−5047; c) O. Schuster, L. Yang, H. G. Raubenheimer, M. Albrecht, *Chem. Rev.* **2009**, *109*, 3445−3478.

[4] M. Melaimi, R. Jazzar, M. Soleilhavoup, G. Bertrand, *Angew. Chem.* **2017**, *129*, 10180-10203; *Angew. Chem. Int. Ed.* **2017**, *56*, 10046-10068.

[5] a) T. Dröge, F. Glorius, *Angew. Chem.* **2010**, *122,* 7094–7107; *Angew. Chem. Int. Ed.* **2010**, *49*, 6940-6952; b) M. N. Hopkinson, C. Richter, M. Schedler, F. Glorius, *Nature* **2014**, *510*, 485−496.

[6] M. Scholl, S. Ding, C. W. Lee, R. H. Grubbs, *Org. Lett.* **1999**, *1*, 953−956.

[7] M. S. Viciu, R. M. Kissling, E. D. Stevens, S. P. Nolan, *Org. Lett.* **2002**, *4*, 2229−2231.

[8] a) M. S. Viciu, R. F. Germaneau, O. Navarro-Fernandez, E. D. Stevens, S. P. Nolan, *Organometallics* **2002**, *21*, 5470−5472; b) N. Marion, O. Navarro-Fernandez, J. Mei, E. D. Stevens, N. M. Scott, S. P. Nolan, *J. Am. Chem. Soc.* **2006**, *128*, 4101−4111.

[9] a) C. J. O'Brien, E. A. Kantchev, C. Valente, N. Hadei, G. A. Chass, A. Lough, A. C. Hopkinson, M. G. Organ, *Chem. Eur. J.* **2006**, *12*, 4743-4748; b) M. G. Organ, M. Abdel-Hadi, S. Avola, I. Dubovyk, N. Hadei, E. A. B. Kantchev, C. J. O'Brien, M. Sayah, C. Valente, *Chem. Eur. J.* **2008**, *14*, 2443−2452; c) T. Tu, W. Fang, J. Jiang, *Chem. Commun.* **2011**, *47*, 12358−12360

[10] a) N. Kuhn, H. Bohnen, J. Kreutzberg, D. Bläser, R. Boese, *J. Chem. Soc., Chem. Commun.* **1993**, 1136−1137; b) N. Kuhn, H. Bohnen, D. Bläser, R. Boese, *Chem. Ber.* **1994**, *127*, 1405−1407; c) For a related study on triazolylidene-based NHOs, see: D. Enders, K. Breuer, G. Raabe, J. Runsink, J. H. Teles, J.–P. Melder, K. Ebel, S. Brode, *Angew. Chem.* **1995**, *107;* 1119-1122; *Angew. Chem., Int. Ed. Engl.* **1995**, *34*, 1021−1023.

[11] M. M. D. Roy, E. Rivard, *Acc. Chem. Res.* **2017**, *50*, 2017-2025.

[12] a) A. Fürstner, M. Alcarazo, R. Goddard, C. W. Lehmann, *Angew. Chem.* **2008**, *120,* 3254 –3258; *Angew. Chem. Int. Ed.* **2008**, *47*, 3210-3214; b) S. M. I. Al-Rafia, A. C. Malcolm, S. K. Liew, M. J. Ferguson, R. McDonald, E. Rivard, *Chem. Commun.* **2011**, *47*, 6987–6989; c) C. E. I. Knappke, A. J. Arduengo III, H. Jiao, J. M. Neudörfl, A. Jacobi von Wangelin, *Synthesis* **2011**, *23*, 3784–3795.

[13] K. Powers, C. Hering-Junghans, R. McDonald, M. J. Ferguson, E. Rivard, *Polyhedron* **2016**, *108*, 8−14.

[14] S. Kronig, P. G. Jones, M. Tamm, *Eur. J. Inorg. Chem.* **2013**, 2301−2314.

[15] a) M. Iglesias, A. Iturmendi, P. J. Sanz Miguel, V. Polo, J. J. Pérez-Torrente, L. A. Oro, L. A. *Chem. Commun.* **2015**, *51*, 12431−12434; b)

A. Iturmendi, N. García, E. A. Jaseer, J. Munárriz, P. J. Sanz Miguel, V. Polo, M. Iglesias, L. A. Oro, *Dalton Trans.* **2016**, *45*, 12835−12845.

[16] a) S. M. I. Al-Rafia, M. J. Ferguson, E. Rivard, *Inorg. Chem.* **2011**, *50*, 10543-10545; b) S. M. I. Al-Rafia, M. R. Momeni, M. J. Ferguson, R. McDonald, A. Brown, E. Rivard, *Organometallics* **2013**, *32*, 6658−6665; c) Y. Wang, M. Y. Abraham, R. J. Gilliard Jr., D. R. Sexton, P. Wei, G. H. Robinson, *Organometallics* **2013**, *32*, 6639-6642; d) C. J. Berger, G. He, C. Merten, R. McDonald, M. J. Ferguson, E. Rivard, *Inorg. Chem.* **2014**, *53*, 1475-1486; e) R. S. Ghadwal, C. J. Schürmann, F. Engelhardt, C. Steinmetzger, *Eur. J. Inorg. Chem.* **2014**, 4921−4926; f) W.-H. Lee, Y.-F. Lin, G.-H. Lee, S.-M. Peng, C.-W. Chiu, *Dalton Trans.* **2016**, *45*, 5937−5940; g) C. Hering-Junghans, P. Andreiuk, M. J. Ferguson, R. McDonald, E. Rivard, *Angew. Chem.* **2017**, *129,* 6368−6372; *Angew. Chem. Int. Ed.* **2017**, *56*, 6272−6275; h) A. Causero, H. Elsen, J. Pahl, S. Harder, *Angew. Chem.* **2017**, *129,* 7010–7014; *Angew. Chem. Int. Ed.* **2017**, *56*, 6906–6910.

[17] For recent examples, see: a) Q. Wang, W. Zhao, S. Zhang, J. He, Y. Zhang, E. Y.-X. Chen, *ACS Catal.* **2018**, *8*, 3571-3578; b) P. Walter, S. Naumann, *Macromolecules* **2017**, *50*, 8406-8416; c) C. Hering-Junghans, I. C. Watson, M. J. Ferguson, R. McDonald, E. Rivard, *Dalton Trans.* **2017**, *46*, 7150-7153; d) U. Kaya, U. P. N. Tran, D. Enders, J. Ho, T. V. Nguyen, *Org. Lett.* **2017**, *19*, 1398-1401.

[18] R. D. Crocker, T. V. Nguyen, *Chem. Eur. J.* **2017**, *22*, 2208-2213.

[19] C. E. I. Knappke, J. M. Neudörfl, A. Jacobi von Wangelin, *Org. Biomol. Chem.* **2010**, *8*, 1695−1705.

[20] For a related fulvalene-type NHOs, see: D. Kunz, E. Ø. Johnsen, B. Monsler, F. Rominger, *Chem. Eur. J.* **2008**, *14*, 10909-10914.

[21] A. Schumann, C. Hering-Junghans, *Eur. J. Inorg. Chem.* **2018**, 2584-2588.

[22] M. Gasperini, F. Ragaini, S. Cenini, *Organometallics* **2002**, *21*, 2950-2957.

[23] For full crystallographic and computational details, see the Supporting Information. CCDC 1903754-1903764 contain the supplementary crystallographic data for this paper. These data are provided free of charge by The Cambridge Crystallographic Data Centre.

[24] R. S. Ghadwal, S. O. Reichmann, F. Engelhardt, D. M. Andrada, G Frenking, *Chem. Commun.* **2013**, *49*, 9440-9442.

[25] R. Schuldt, J. Kästner, S. Naumann, *J. Org. Chem.* **2019**, *84*, 2209–2218.

[26] M. Lesieur, A. M. Z. Slawin, C. S. Cazin, *Org. Biomol. Chem.* **2014**, *12*, 5586−5589.

[27] a) K. H. Hoi, J. A. Coggan, M. G. Organ, *Chem. Eur. J.* **2013**, *19*, 843-845; b) M. Pompeo, J. L. Farmer, R. D. J. Froese, M. G. Organ, *Angew. Chem.* **2014**, *126*, 3287-3290; *Angew. Chem. Int. Ed.* **2014**, *53,* 3223-3226; c) S. Sharif, R. P. Rucker, N. Chandrasoma, D. Mitchell, M. J. Rodriquez, R. D. J. Froese, M. G. Organ, *Angew. Chem.* **2015**, *127*, 9643-9647; *Angew. Chem. Int. Ed.* **2015**, *54*, 9507-9511.

[28] D. S. Surry, S. L. Buchwald, *Chem. Sci.* **2011**, *2*, 27-50.

[29] R. H. Crabtree, *Chem. Rev.* **2012**, *112*, 1536-1554.

[30] O. N. Gorunova, I. M. Novitskiy. Y. K. Grishin, I. P Gloriozov, V. A. Roznyatovsky, V. N. Khrustalev, K. A. Kochetkov, V. V. Dunina, *Organometallics* **2018**, *37*, 2842-2858.

[31] C. S. Higman, A. E. Lanterna, M. L. Marin, J. C. Scaiano, D. E. Fogg, *ChemCatChem* **2016**, *8*, 2446-2449.

[32] M. A. Watzky, R. G. Finke, *J. Am. Chem. Soc.* **1997**, *119*, 10382-10400.

[33] The Finke-Watzky model works on the assumption that the step which consumes the reagent being monitored (in this case 9-bromoanthracene) is fast compared to the rate of nanoparticle formation. Since the model fits reasonably well with our data, we can state that the Buchwald-Hartwig amination occurring is faster than the formation of catalytically active nanoparticles.

[34] D. S. McGuinness, N. Saendig, B. F. Yates, K. J. Cavell, *J. Am. Chem. Soc.* **2001**, *123*, 4029-4040.

[35] V. Sable, K. Maindan, A. R. Kapdi, P. S. Shejwalker, K. Hara, *ACS Omega* **2017**, *2*, 204-217.

[36] S. Navaladian, B. Viswanathan, T. K. Varadarajan, R. P. Viswanath, *Nanoscale Res. Lett.* **2009**, *4*, 181-186.

[37] A. J. Arduengo III, R. Krafczyk, R. Schmutzler, H. A. Craig, J. R. Goerlich, W. J. Marshall, M. Unverzagt, *Tetrahedron* **1999**, *55*, 14523-14534.

[38] S. Gaillard, X. Bantreil, A. M. Z. Slawin, S. P. Nolan, *Dalton Trans.* **2009**, *35*, 6967-6971.

[39] K. V. Vasudevan, R. R. Butorac, C. D. Abernathy, A. H. Cowley, *Dalton Trans.* **2010**, *39*, 7401-7408.

[40] X. Bantriel; S. P. Nolan, *Nat. Protoc.* **2011**, *6*, 69-77.

[41] S. J. Ryan, S. D. Schimler, D. C. Bland, M. S. Sanford, *Org. Lett.* **2015**, *17,* 1866-1869.

[42] G. M. Sheldrick, *Acta. Crystallogr. Sect. A* **2015**, *71*, 3–8.

[43] G. M. Sheldrick, *Acta. Crystallogr. Sect. C* **2015**, *71*, 3–8.

[44] Gaussian 09, Revision E.01, M. J. Frisch, G. W. Trucks, H. B. Schlegel, G. E. Scuseria, M. A. Robb, J. R. Cheeseman, G. Scalmani, V. Barone, B. Mennucci, G. A. Petersson, H. Nakatsuji, M. Caricato, X. Li, H. P. Hratchian, A. F. Izmaylov, J. Bloino, G. Zheng, J. L. Sonnenberg, M. Hada, M. Ehara, K. Toyota, R. Fukuda, J. Hasegawa, M. Ishida, T. Nakajima, Y. Honda, O. Kitao, H. Nakai, T. Vreven, J. A. Montgomery, Jr., J. E. Peralta, F. Ogliaro, M. Bearpark, J. J. Heyd, E. Brothers, K. N. Kudin, V. N. Staroverov, R. Kobayashi, J. Normand, K. Raghavachari, A. Rendell, J. C. Burant, S. S. Iyengar, J. Tomasi, M. Cossi, N. Rega, J. M. Millam, M. Klene, J. E. Knox, J. B. Cross, V. Bakken, C. Adamo, J. Jaramillo, R. Gomperts, R. E. Stratmann, O. Yazyev, A. J. Austin, R. Cammi, C. Pomelli, J. W. Ochterski, R. L. Martin, K. Morokuma, V. G. Zakrzewski, G. A. Voth, P. Salvador, J. J. Dannenberg, S. Dapprich, A. D. Daniels, Ö. Farkas, J. B. Foresman, J. V. Ortiz, J. Cioslowski, D. J. Fox, Gaussian, Inc., Wallingford CT, 2009.

[45] A. D. Becke, *J. Chem. Phys.* **1993**, *98*, 5648-5652.

[46] a) G. A. Petersson, A. Bennett, T. G. Tensfeldt, M. A. Al-Laham, W. A. Shirley, J. Mantzaris, *J. Chem. Phys.* **1988**, *89*, 2193-2218; b) G. A. Petersson, M. A. Al-Laham, *J. Chem. Phys.* **1991**, *94*, 6081-6090.

[47] a) E. D. Glendening, J. K. Badenhoop, A. E. Reed, J. E. Carpenter, J. A. Bohmann, C. M. Morales, C. R. Landis, F. Weinhold, *NBO 6.0*, Theoretical Chemistry Institute, University of Wisconsin, Madison, **2013**; b) J. E. Carpenter, F. Weinhold, *J. Mol. Struct.: THEOCHEM* **1988**, *169*, 41–62; c) F. Weinhold, J. E. Carpenter, *The Structure of Small Molecules and Ions*, Plenum Press, **1988**; d) F. Weinhold, C. R. Landis, *Valency and Bonding. A Natural Bond Orbital Donor- Acceptor Perspective*, Cambridge University Press, **2005**.

Layout 2:

FULL PAPER

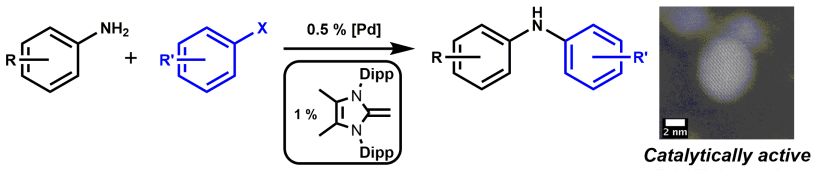

Catalytically active Pd-NP formation

***N*-Heterocyclic olefins** (NHOs) with functionalized backbones and modifications to the terminal alkylidene positions are described. Various Pd(II)-NHO complexes have been synthesized and their effectiveness as pre-catalysts in Buchwald-Hartwig aminations was explored. Evidence suggests that catalysis is mediated by colloidal palladium metal, which highlights the different coordination ability of NHOs in comparison with the commonly used *N*-heterocyclic carbene co-ligands.

Ian C. Watson, André Schumann, Haoyang Yu, Prof. Dr. Emma C. Davy, Dr. Robert McDonald, Dr. Michael J. Ferguson, Prof. Dr. Christian Hering-Junghans, Prof. Dr. Eric Rivard,**

Page xx. – Page xx

_N_-Heterocyclic Olefin Ligated Palladium(II) Complexes as Pre-Catalysts for Buchwald-Hartwig Aminations